Millennial-scale variability in the local radiocarbon reservoir age of south Florida during the Holocene

Lauren T. Toth[1*], Hai Cheng[2,3], R. Lawrence Edwards[2], Erica Ashe[4], Julie N. Richey[1]

[1]U.S. Geological Survey, St. Petersburg Coastal and Marine Science Center, 600 Fourth Street South, Saint Petersburg, FL 33701, USA

[2]Department of Earth Sciences, University of Minnesota, Minneapolis, MN 55455, USA

[3]Institute of Global and Environmental Change, Xi'an Jiaotong University, Xi'an 310049, China

[4]Department of Statistics and Biostatistics, Rutgers University, 110 Frelinghuysen Rd., Piscataway, NJ 08854, USA

*Corresponding author: ltoth@usgs.gov

Abstract

A growing body of research suggests that the marine environments of south Florida provide a critical link between the tropical and high-latitude Atlantic. Changes in the characteristics of water masses off south Florida may therefore have important implications for our understanding of climatic and oceanographic variability over a broad spatial scale; however, the sources of variability within this oceanic corridor remain poorly understood. Measurements of ΔR, the local offset of the radiocarbon reservoir age, from shallow-water marine environments can serve as a powerful tracer of water-mass sources that can be used to reconstruct variability in local- to regional-scale oceanography and hydrology. We combined radiocarbon and U-series measurements of Holocene-aged corals from the shallow-water environments of the Florida Keys reef tract (FKRT) with robust statistical modeling to quantify the millennial-scale variability in ΔR at locations with ("nearshore") and without ("open ocean") substantial terrestrial influence. Our reconstructions demonstrate that there was significant spatial and temporal variability in ΔR on the FKRT during the Holocene. Whereas ΔR was similar throughout the region after ~4000 years ago, nearshore ΔR was significantly higher than in the open ocean during the middle Holocene. We suggest that the elevated nearshore ΔR from ~8000–5000 years ago was most likely the result of greater groundwater influence associated with lower sea level at this time. In the open ocean, which was isolated from the influence of groundwater, ΔR was lowest ~7000 years ago, and was highest ~3000 years ago. We evaluated our open-ocean model of ΔR variability against records of local- to regional-scale oceanography and conclude that local upwelling was not a significant driver of open-ocean radiocarbon variability in this region. Instead, the millennial-scale trends in open-ocean ΔR were more likely a result of broader-scale changes in western Atlantic circulation associated with an increase in the supply of equatorial South Atlantic water to the Caribbean and shifts in the character of South Atlantic waters resulting from variation in the intensity of upwelling off the southwest coast of Africa. Because accurate estimates of ΔR are critical to precise calibrations of radiocarbon dates from marine samples, we also developed models of nearshore and open-ocean ΔR versus conventional ^{14}C ages that can be used for regional radiocarbon calibrations for the Holocene. Our study provides new insights into the patterns and drivers of oceanographic and hydrologic variability in the Straits of Florida and highlights the value of the paleoceanographic records from south Florida to our understanding of Holocene changes in climate and ocean circulation throughout the Atlantic.

Key words: ΔR, radiocarbon, Holocene, circulation, western Atlantic, upwelling, groundwater

1. Introduction

The oceanic corridor between the Florida Keys and Cuba, known as the Straits of Florida, provides a critical connection between the tropical and high-latitude western Atlantic (Fig. 1; Hall and Bryden, 1982; Schmitz and Richardson, 1991; Schmitz and McCartney, 1993; Lee et al., 1995; Lund and Curry, 2004; Lynch-Stieglitz et al., 2009; Schmidt et al., 2012;). Flow through the Straits of Florida occurs via the Florida Current, which is formed by the confluence of the Gulf of Mexico Loop Current and the eastward extension of the Yucatan Current from the southern Caribbean. (Fig. 1b; Schmitz and Richardson, 1991; Lee et al., 1995). The Florida Current is situated at the origin of the Gulf Stream, which is the primary mechanism of heat and salt transport to the North Atlantic (Hall and Bryden, 1982; Schmitz and McCartney, 1993; Lee et al., 1995; Lund and Curry, 2006). Variations in the sources and character of the Florida Current may, therefore, have important implications for Atlantic Ocean circulation and regional climate variability (Lynch-Stieglitz et al., 1999; Lund and Curry, 2006; Came et al., 2008; Schmidt et al., 2012).

Recent studies have demonstrated that there were considerable changes in the hydrography (Lund and Curry, 2004, 2006; Lynch-Stieglitz et al., 2009; Schmidt et al., 2012) and geostrophic flow through the Straits of Florida during the Holocene (Lund et al., 2006; Lynch-Stieglitz et al., 2009). These changes have been linked to large-scale climate phenomena including solar forcing (Lund and Curry, 2004, 2006; Lynch-Stieglitz et al., 2009; Schmidt et al., 2012), meridional shifts in the position of the inter-tropical convergence zone (Lund and Curry, 2004; Lund et al., 2006; Lynch-Stieglitz et al., 2009), Atlantic Meridional Overturning Circulation (AMOC; Lund et al., 2006; Lynch-Stieglitz et al., 2007; Came et al., 2008; Lynch-Stieglitz et al., 2009), and the El Niño–Southern Oscillation (Schmidt et al., 2012); however, the local- to regional-scale oceanographic responses to climate forcing and the role of ocean circulation in determining the characteristics of the Florida Current are less clear.

Radiocarbon (^{14}C) variability in shallow-water environments can provide a powerful tracer of changes in ocean circulation through space and time (Broecker et al., 1960; Druffel, 1997b). The ^{14}C content of the oceanic mixed layer reflects both variability in atmospheric ^{14}C

production and exchange with ^{14}C-depleted sources (Broecker et al., 1960; Stuiver et al., 1986; Reimer and Reimer, 2001). On a global scale, mixing with ^{14}C-depleted deepwater produces a significant offset between the ^{14}C of the atmosphere and marine surface-water, known as the global marine radiocarbon reservoir age, R, which is modeled over time by the marine calibration curve (e.g., Reimer et al., 2013). Local- to regional-scale oceanographic or hydrologic variability can, however, produce significant local deviations from this globally-averaged value (e.g., Druffel and Linick, 1978; Druffel, 1997a; Reimer and Reimer, 2001; Guilderson et al., 2004; Kilbourne et al., 2007; Druffel et al., 2008; Wagner et al., 2009; Dewar et al., 2012; Toth et al., 2015a, b). The local offset of the radiocarbon reservoir age at any given location is known as the local reservoir age correction, ΔR (Stuiver et al., 1986; Reimer and Reimer, 2001).

At present, the most significant source of local oceanographic variability in the Straits of Florida is periodic upwelling of intermediate water as the result of cyclonic gyres and offshore meanders of the Florida Current (Klein and Orlando, 1994; Lee et al., 1995; Leichter and Miller, 1999; Davis et al., 2008; Fig. 1c). From Dry Tortugas N.P. to the Lower Keys (Fig. 1c), periodic formation of large, slow-moving cyclonic gyres is an important inter- and intra-annual driver of water-column mixing (Klein and Orlando, 1994; Lee et al., 1995). High-frequency, but short-lived upwelling is a persistent feature in the Upper Keys where the Florida Current flows closest to the reef tract (Klein and Orlando, 1994; Leichter and Miller, 1999). The upwelling regime of south Florida over longer timescales is unknown, but significant changes in the intensity or frequency of upwelling should be reflected in ΔR variability. Because ΔR is a function of mixing, upwelling results in surface-water with depleted ^{14}C and elevated ΔR, and the opposite occurs where there is strong water-column stratification or downwelling (Broecker et al., 1960; Key et al., 2004; Reimer and Reimer, 2001).

Terrestrial influences from the Florida platform are another potential source of local-scale ΔR variability in the Straits of Florida. Terrestrially-derived sediments, runoff of meteoric waters, and groundwater contributions can all influence the apparent age of nearshore water masses (Pearson and Hanshaw, 1971; Cowart et al., 1978; Böhlke et al., 1999; Porcelli and Swarzenski, 2003; Rosenheim et al., 2007; Swarzenski, 2007; Clark et al., 2014). The contribution of submarine groundwater, which flows freely though the highly-porous carbonates of the Florida platform (Cowart et al., 1978; Corbett et al., 1999), is thought to be especially important in the nearshore marine environments of south Florida (Shinn et al., 1994; Corbett et al., 1999; Plummer and Sprinkle, 2001; Reich et al., 2002; Chanton et al., 2003; Reich et al., 2006). The limestones that comprise Florida's subterranean aquifers, and the Pleistocene platform that transports groundwater seaward, are significantly older than the water masses they contain (Pearson and Hanshaw, 1971; Böhlke et al., 1999; Plummer and Sprinkle, 2001; Reich et al. 2006). Dissolution of these ^{14}C-depleted carbonates results in anomalously old apparent radiocarbon ages of Florida's groundwater (Pearson and Hanshaw, 1971; Böhlke et al., 1999; Plummer and Sprinkle, 2001). Although the groundwater that reaches south Florida's Atlantic coast is likely a mixture of isolated water masses from the Florida aquifers and seawater from the Florida Bay and Biscayne Bay (Böhlke et al., 1999; Reich et al. 2002, 2006), significant groundwater input to south Florida's marine environments could result in elevated ΔR.

The signature of local oceanography and hydrology on ΔR variability in south Florida may also be overprinted by larger-scale changes in circulation. The water masses that enter the Caribbean Basin via the Caribbean Current have both South and North Atlantic origins (Fig. 1a,b; Schmitz and Richardson, 1991; Wilson and Johns, 1997; Kilbourne et al., 2007) and the relative contribution of these sources may vary over intra-annual to millennial timescales (Johns et al., 2002; Kilbourne et al., 2007). Whereas subtropical water masses originating in the North Atlantic have relatively high ^{14}C, water masses from the South Atlantic are depleted in ^{14}C due to upwelling of water off the western coast of Africa (Fig. 1a; Southon et al., 2002; Key et al., 2004; Kilbourne et al., 2007; Lewis et al., 2008; Dewar et al., 2012). Because the Florida Current is the terminus of Caribbean circulation, changes in ΔR in the Straits of Florida could reflect the relative contributions of equatorial versus subtropical water masses to the Caribbean, as well as the character of those water masses, through time (c.f., Kilbourne et al., 2007).

Determining the influence of local- versus regional-scale controls on the oceanographic and hydrologic variability of south Florida is crucial to discerning the long-term controls on Florida Current variability and its impacts on larger-scale climatic and oceanographic oscillations. We combined coral-based "snapshots" of ΔR from the shallow-water environments of the Florida Keys using empirical Bayesian modeling to reconstruct regional oceanographic and hydrological variability during the Holocene. Spatial gradients in the hydrology of the marine environments of south Florida led us to develop two distinct ΔR reconstructions for locations with and without significant terrestrial influence: "nearshore" and "open-ocean" locations, respectively. We first evaluate the potential drivers of ΔR millennial-scale variability in nearshore environments. We then compare the trends in open-ocean ΔR to existing paleoceanographic reconstructions, to evaluate the relative contributions of local upwelling versus regional-scale changes in ocean circulation to oceanographic variability in the Straits of Florida.

2. Regional Setting

The Florida Keys Reef Tract (FKRT) is located 6–10 km seaward of the exposed islands of the Florida Keys, from Biscayne National Park (N.P.) in the northeast, to Dry Tortugas N.P. in the southwest (Fig. 1c). Regional oceanography of the FKRT is driven by the dynamics of the Florida Current, which parallels the reef tract through the Straits of Florida (Fig. 1b; Klein and Orlando, 1994); however, the FKRT can be divided into six subregions based on hydrological, ecological, and geological variability (Ginsburg and Shinn, 1994; Klein and Orlando, 1994): Biscayne N.P., the Upper Keys, the Middle Keys, the Lower Keys, the Marquesas, and Dry Tortugas N.P. (Fig. 1c).

Whereas Dry Tortugas N.P. and the Marquesas are generally considered to be open-ocean environments, the other subregions are strongly influenced by the regional hydrology of south Florida (Klein and Orlando, 1994). In the Middle Keys, large passes between the islands allow for tidal transport of surface water from Florida Bay onto the reef (Ginsburg and Shinn, 1994; Reich et al., 2002). Because Florida Bay is a shallow-water platform with restricted circulation, surface waters in the Bay experience extreme variability in water temperature, salinity, and nutrients (Ginsburg and Shinn, 1994; Klein and Orlando, 1994; Precht and Miller, 2007; Toth et al., 2016). Tidal transport of surface waters from Biscayne Bay has similar impacts on the reefs in that subregion (Reich et al. 2006; Ginsburg and Shinn, 1994; Precht and Miller, 2007). Tidal pumping also facilitates regional submarine groundwater flow, (Reich et al., 2002; Chanton et al., 2003), which is likewise characterized by elevated nutrients and salinity extremes (Shinn et al., 1994; Corbett et al., 1999). The frequent intrusion of these water masses can result in highly variable conditions on the reefs of the Lower, Middle, and Upper Keys and Biscayne N.P. subregions (Klein and Orlando, 1994; Reich et al., 2006). The high variability in the hydrology and oceanography of this region at present suggests that environmental variability may have also had a significant impact on the FKRT over millennial timescales.

3. Materials and Methods

3.1 Sample Description

The U.S. Geological Survey Coastal and Marine Science Center in Saint Petersburg, Florida houses an extensive collection of Holocene reef cores collected from throughout the FKRT over the past 50 years (Fig. 1c; Reich et al., 2012; http://olga.er.usgs.gov/coreviewer/). In the present study, we sampled corals from 41 cores across the six subregions of the FKRT (Dry Tortugas N.P.=6, Marquesas=3, Lower Keys=7, Middle Keys=7, Upper Keys=9, Biscayne N.P.=9). All cores were collected from shelf-edge reefs at ~0–15 m depth below mean sea level. We used existing radiocarbon ages from the cores (e.g., Reich et al., 2006, 2009; Brock et al., 2010) to select samples that would provide the highest temporal resolution for each subregion. We note, however, that reef development across most of the FKRT did not initiate until after ~8000 yrs BP (Shinn et al. 1977) and we did not have any samples from the open-ocean sites before that time. Similarly, reef development was negligible throughout the FKRT after ~4000 yrs BP (Shinn et al. 1977), and we were unable to obtain any samples from ~4500–3000 yrs BP from the Keys and Biscayne N.P. subregions.

We sampled 68, visually-unaltered sub-fossil corals from five genera in the cores: Dry Tortugas N.P.=19, Marquesas=4, Lower Keys=11, Middle Keys=9, Upper Keys=14, and Biscayne N.P.=11 (Table 1). The samples, which represented ~1–3 years in the growth history of the coral, were cut from clean, visually unaltered sections of the corals using a tile saw. Each sample was cut into two, ~1–2 g subsamples, which were sonicated in a bath of warm deionized water and dried at 60°C prior to U-series and radiocarbon analysis.

3.2 Dating

All but two coral samples were processed at the USGS Radiocarbon Laboratory in Reston, VA and were radiocarbon dated using accelerator mass spectrometry (AMS) at the Center for AMS at Lawrence Livermore National Laboratory. We report conventional ^{14}C ages, which were previously corrected for fractionation of ^{13}C. The $\delta^{13}C$ of those samples was either measured by University of California, Davis Stable Isotope Laboratory or, if not measured, were assumed to be 0±3‰ (Törnqvist et al., 2015). The other two samples were dated previously (Lidz et al., 2003; Toth et al., 2017) using radiometric radiocarbon dating at Beta Analytic, Inc. or Geochron Laboratories. Conventional radiocarbon ages are reported in Table 1 and the complete radiocarbon dataset, including fraction modern (Fm) for the AMS ages, is available at https://doi.org/10.5066/F7P8492Q.

U-series ages were determined at the University of Minnesota and Xi'an Jiaotong University using multicollector inductively coupled plasma mass spectrometry according to the procedures described in Cheng et al. (2013). Measured ^{230}Th ages were corrected using an initial $^{230}Th/^{232}Th$ atomic ratio of 4.4×10^{-6} with an uncertainty of 50% (±2.2). Corrected ^{230}Th ages are reported in Table 1 and the complete U-series dataset is available at https://doi.org/10.5066/F7P8492Q.

3.3 Data Screening

None of the samples included in this study had any visible evidence of alteration; however, we performed additional diagenetic screening and critical evaluation of the U-series data to ensure that all of the samples included in our final reconstruction were pristine. Although we were unable to use X-ray diffraction (XRD) to screen the corals for diagenesis in the present study, sixteen of the corals were previously screened using a Bruker D4 XRD (Reich et al., 2009;

Toth et al., 2017). These analyses indicated that all samples contained <5% calcite (the % calcite in the reference sample) and, in most cases, the samples were nearly 100% aragonite (Reich et al., 2009; Toth et al., 2017). We screened an additional sub-sample (N=14) of corals, using the S-3500N Hitachi scanning electron microscope (SEM) housed at the University of South Florida's College of Marine Science. We chose corals from throughout the Holocene and from all six regions for screening by SEM, but preferentially included any corals that produced ΔR values that were in disagreement with adjacent samples in the record to ensure that altered samples would not bias the reconstruction. Only one sample (BP-FR-2-55) had evidence of localized calcite cements (Fig. A1). Although the sample was dated, it was excluded from further analysis because it also contained anomalously high ^{238}U (see below). Only two additional samples were removed from the dataset because of significant diagenesis: a coral from the Middle Keys (MK-AR-2-0), which had extensive formations of secondary aragonite, and one from Lower Keys (LK-MG-2-0) that had moderate amounts of secondary aragonite and evidence of widespread dissolution (Fig. A1). SEM imaging of the remaining samples showed only the localized presence of secondary aragonite and suggested that diagenetic alteration was negligible overall (i.e., >1% of the imaged area of the coral; Figs. A2–A5; Toth et al., 2017).

Careful screening of the U-series data led us to exclude 13 corals from the dataset (BP-FR-2-55 and 12 additional samples). One sample from Dry Tortugas N.P. (DT-GB-1-12) and one from the Upper Keys (UK-CF-1-15) were excluded because low $^{230}Th/^{232}Th$ indicated that there was a possibility of inherited (non-radiogenic) ^{230}Th (Cobb et al., 2003; Clark et al., 2014). Eleven additional corals had ^{238}U values outside the ranges typically reported for their respective genera: ~2800–3800 ppb for *Acropora* spp. and ~2000–3200 for the massive coral taxa *Orbicella* spp., *Diploria* spp., *Montastraea cavernosa*, and *Colpophyllia natans* (Cross and Cross, 1983;

Muhs et al., 2011). These samples were excluded from further analysis because elevated (low) ^{238}U suggests the possibility of uranium gain (loss).

The 15 samples that were excluded from further analysis as a result of our diagenetic and U-series screening procedures are highlighted in red in Table 1. A summary of the screening is also provided at https://doi.org/10.5066/F7P8492Q (Toth et al., 2017). One sample (MK-AR-7-0), which passed our screening procedures (U-series and SEM), represented an extreme outlier in our ΔR dataset (ΔR=399±29). Although we include this anomalous value in our results, we excluded it from the statistical models because it would have caused a biasing that we could not attribute with any certainty to real hydrologic or oceanographic variability.

Ultimately, we included 53 of the 68 original estimates of ΔR in our models. We divide these records into two distinct datasets, nearshore (<10 km from the Florida Keys and <100 km from mainland Florida) and open ocean (>10 km from the Florida Keys and >100km from mainland FL), based on the unique hydrology and environmental history of the sites. Whereas we assume that the open-ocean environments of Dry Tortugas N.P. and the Marquesas had little or no terrestrial influences during the Holocene, the regional hydrology of south Florida may have significantly influenced ΔR variability in the Keys and Biscayne N.P. subregions. The open-ocean reconstruction includes 20 records of ΔR: 16 from the Dry Tortugas N.P. and four from the Marquesas. The nearshore reconstruction includes 32 records of ΔR: six from the Lower Keys, six from the Middle Keys, 13 from the Upper keys, and seven from Biscayne N.P. We note that estimates of ΔR from previous analyses of modern (Lighty et al., 1982; Druffel and Linick, 1978; Druffel, 1997b) and middle Holocene corals (Druffel et al., 2008) were not included in our reconstructions because the differences in the values (i.e., Lighty et al., 1982) or the resolution of the data (i.e., Druffel and Linick, 1978; Druffel, 1997b; Druffel et al., 2008) had the potential to bias our statistical model; however, we do compare these data to our reconstuctions in the discussion of our results.

3.4 Determination of ΔR

ΔR is calculated by determining the offset between the measured and predicted radiocarbon age at a given point in time (Stuiver et al., 1986; Reimer and Reimer, 2001). Using the U-series ages as the “true” ages, we determined the expected ^{14}C age of each sample from the Marine13 calibration curve (Reimer et al., 2013). ΔR was then calculated by subtracting the expected ^{14}C age from the conventional ^{14}C age of each sample. We computed a combined error term for ΔR by taking the root-mean-square of the errors associated with the conventional and expected ^{14}C ages (Stuiver et al., 1986). Each estimate of ΔR represents a discrete “snapshot” of the radiocarbon age of the local surface water. We compared the snapshots of ΔR between the nearshore sites and the open-ocean sites using a general linear model analysis of variance (glm-ANOVA) using R version 3.1.1 (R Core Team, 2014). The data residuals of the model were approximately normally-distributed (Shaprio-Wilk: W= 0.96, p=0.09) and the data conformed to the assumption of homogeneity of variance (Levene’s Test: $F_{1,50}$=0.01, p=0.92).

3.5 Statistical Modeling of ΔR through time

Using a simplification of the method described in Khan et al. (2017) and Kopp et al. (2016), we combined the coral-based snapshots of ΔR using empirical hierarchical models with Gaussian process priors to 1) reconstruct temporal variability in ΔR during the Holocene (ΔR versus ^{230}Th ages) and 2) predict values of ΔR and ΔR uncertainty for use in calibrations of radiocarbon ages from the region (ΔR versus conventional ^{14}C ages) for both the open-ocean and nearshore sites. The hierarchical model level divides into a data level, a process level, and a hyperparameter level.

At the data level, we observe noisy ΔR, $d\mathrm{R}_i$, and noisy age term, $\hat{t_i}$, which is either derived from the ^{230}Th age or the ^{14}C age:

$$d\mathrm{R}_i = \Delta\mathrm{R}(t_i) + \epsilon_i^{\Delta R}$$
$$t_i = \hat{t_i} + \epsilon_i^{t}$$
$$\epsilon_i^{\Delta R} \sim N\{0, (\sigma_i^{\Delta R})^2\}$$
$$\epsilon_i^{t} \sim N\{0, (\sigma_i^{t})^2\}$$

where i indexes the data points, $\Delta\mathrm{R}(t)$ is the true ΔR as a function of t, t_i is the true age (from ^{230}Th) or the conventional ^{14}C age of observation i, $\hat{t_i}$ is the mean observed (^{230}Th or conventional ^{14}C) age, $\epsilon_i^{\Delta R}$ is normally distributed uncertainty or error, with standard deviation given by the root-mean-square error for ΔR, and ϵ_i^{t} is the error in the corrected ^{230}Th or conventional ^{14}C age of the sample. The age uncertainties are incorporated using the noisy-input Gaussian Process (GP) method described in McHutchon and Rasmussen (2011), which uses a first-order Taylor-series approximation to translate errors in the independent variable (age) into equivalent errors in the dependent variable (ΔR):

$$\Delta\mathrm{R}(t_i) \approx \Delta\mathrm{R}(\hat{t_i}) + \epsilon_i^{t} \frac{\partial \Delta\mathrm{R}(\hat{t_i})}{\partial t}$$

At the process level, the prior distribution of ΔR is a mean-zero GP, characterized by hyperparameters that comprise the amplitude $\sigma_{\Delta R}$ and timescale of variability τ,

$$\Delta\mathrm{R}(t) \sim GP\{0, \sigma_{\Delta R}{}^2 \rho(t, t'; \tau)\} + w(t)$$

where ρ is the Matérn correlation function with smoothness parameter $^3/_2$ and scale τ (Rasmussen and Williams, 2006), and $w(t)$ is white noise ($\sim N\{0, (\sigma_w)^2\}$), which captures high-frequency variability in ΔR. The use of a smoothness parameter of $^{3}/_{2}$ ensures that the first derivative of the process will be defined everywhere, but allows for abrupt changes in rate.

The hyperparameters of the model include $\sigma_{\Delta R}$, τ, and σ_w, which are the prior amplitude of variability, the prior amplitude of white noise, and the time scale of variability, respectively. We employ an empirical Bayesian analysis method, in which the hyperparameters are optimized based on the data to maximize the likelihood of the model. The maximum-likelihood point estimates of $\sigma_{\Delta R}$ and τ were conditioned on the data from both the open-ocean and nearshore sites (resulting in values of 38 and 850 years), whereas σ_w was tuned for each model separately (resulting in a value of 20 years for nearshore and 1 year for open ocean) in order to account for different uncertainties in predicted ΔR. The prior is uninformative (with the only assumption being that the errors are Gaussian), where the data determines the best fit of the variability, so that the prior distribution cannot influence the results of the analysis. The key output of the model is an estimate of the posterior probability distribution of ΔR, $\Delta R(t)$, conditional on the tuned hyperparameters. We calculated the rates of change in ΔR based on a linear transformation of $\Delta R(t)$ over 1000 year periods (Fig. B1).

4. Results

4.1 Coral-based snapshots of Holocene ΔR

Our complete dataset of coral-based snapshots of ΔR from the FKRT extend across nearly the entire Holocene epoch from 41–9443 yrs before present (BP; ^{230}Th age) and span the conventional ^{14}C ages of 380–8760 (Table 1). The full range of ΔR over this period is more than 500 years (-157–399); however, excluding the single anomalously high value from the Middle Keys, the maximum value of ΔR was 84±31 years (mean ± 1 standard deviation [SD]; Fig. 2).

The overall range of values was similar between the nearshore sites and open-ocean, but ΔR was generally higher in the nearshore: values ranged -115–84 years (41–9443 years BP) and -157–34 years (156–7910 cal yrs BP) in the nearshore and open ocean, respectively (Table 1).

Even without the significant outlier from the Middle Keys, ΔR was significantly higher on average in nearshore subregions (-22± 56 years) compared with the open-ocean environments (-64±55 years; glm-ANOVA: $F_{1,50}$=7.057, p=0.01). This difference was primarily the result of elevated ΔR in the Keys and Biscayne subregions from ~7000–5000 yrs BP, when ΔR averaged 13±38 years. In contrast, ΔR snapshots from throughout the FKRT were within error of one another during the rest of the Holocene.

4.2 Models of ΔR variability

By accounting for both chronological uncertainties and the error in our estimates of ΔR, the temporal models of ΔR from the nearshore and open-ocean regions of the FKRT provide a probabilistic assessment of spatial and temporal trends in ΔR during the Holocene. The models provide robust representations of the data: predicted values always fall within two standard deviations (2σ) of the coral-based estimates (Fig. 2a,b), and the 2σ of the models generally include the midpoints of the coral-based estimates. For the nearshore locations, the model spans from 9500–0 yrs BP; however, the model from the open-ocean sites only extends to 8000 yrs BP because there was no data from the open-ocean sites before that time.

Our reconstructions suggest that there was significant spatial and temporal variability in ΔR through the Holocene (Fig. 2). Modeled open-ocean ΔR averaged -60±33 years and ranged from -108 to -6 years from 8000 yrs BP to present (Fig. 2a). Modeled ΔR from nearshore environments was generally higher than in the open ocean, averaging -26±19 years and ranging from -57 to 14 years over this same period (Fig. 2b). The nearshore model had more high-frequency variability compared with the open-ocean reconstruction, where the modeled changes in ΔR appeared more systematic (Fig. 2; Fig. B2). Because of the apparent high-frequency variability in nearshore ΔR, the modeled uncertainties associated with this record were higher and, as a result, none the temporal changes in ΔR at this location were statistically significant. In contrast, we were able to detect temporal significant changes in open-ocean ΔR during the Holocene.

Our earliest records, which come from the nearshore environments of the FKRT, suggest that nearshore ΔR was close to zero, -11±35 years, during the early Holocene (9500 yrs BP; Fig. 2b), but declined after this time. In the middle Holocene, from ~8000–4000 yrs BP, the nearshore and open-ocean reconstructions suggest divergent trends in ΔR variability. In the open-ocean, ΔR declined after 8000 yrs BP, reaching the lowest value for the Holocene at ~7200 yrs BP: -108±27 years (Fig. 2a; Fig. B1). During this same period, however, ΔR was rapidly increasing in the nearshore environments of the FKRT (Fig. B1), reaching a peak value of 14±25 years at 6600 yrs BP (Fig. 2b), which was significantly higher than open-ocean ΔR at that time (i.e., the 95% confidence intervals [CIs] of the models do not overlap; Fig. 2c). Whereas ΔR averaged -99±10 years in the open ocean from 7500–5500 yrs BP, nearshore ΔR during that same period averaged just -5±15 years. Both records trended towards more similar values after ~7000 yrs BP (Fig. 2c; Fig. B1); however, nearshore ΔR was still relatively elevated compared with the open ocean for the rest of the middle Holocene.

Although the trends in ΔR from the nearshore and open-ocean environments of the FKRT were distinct during the early and middle Holocene, the reconstructions converged during the late Holocene, after ~4000 yrs BP (Fig. 2a–c; Fig. B1). Both records indicate that there was an increase in ΔR centered around ~3000 yrs BP, with a peak ΔR of -6 at both locations (±33 in the nearshore locations and ±26 in the open-ocean). Open-ocean ΔR was significantly higher at ~3000 yrs BP than at ~7000 yrs BP when open-ocean ΔR was lowest (based on the 95% CIs of the model; Fig. 2a). The trend of increasing ΔR throughout the FKRT after ~5000 yrs BP is also supported by the similarity between our reconstruction of nearshore ΔR and Druffel et al.'s (2008) reservoir ages from mid-Holocene (~4955–4910 yrs BP) and late Holocene (~3065–3010 yrs BP) corals from Biscayne N.P. (values from Druffel et al. [2008] re-calculated using Marine13: ΔR=-29±39 and -19±38; average modeled values: ΔR=-17±30 and -6±32).

ΔR generally declined throughout the FKRT from ~2500–2000 yrs BP and averaged -45±7 and -52±6 from 2000 yrs BP to present at the nearshore and open-ocean locations, respectively. Our models predict a modern (1950 C.E.) ΔR of -54±32 years and -64±27 years for the nearshore and open-ocean locations, respectively. Similar trends were observed in the models of ΔR versus conventional ^{14}C age (Fig. B2; Toth et al. 2017).

5. Discussion

Our reconstructions demonstrate that there was considerable local variability in the ΔR of shallow marine environments of south Florida during the Holocene, with values ranging over 100 years in the open-ocean and more than 70 years in the nearshore (Fig. 2). In the open-ocean environments, ΔR increased significantly from ~7000 to ~3000 yrs BP before declining to more moderate values at present (Fig. 2a). Although the trends in nearshore ΔR were similar to the open-ocean during the late Holocene, ΔR was significantly higher in the nearshore during the middle Holocene (Fig 2b,c). We hypothesize that during the middle Holocene, the signature of oceanic ΔR in nearshore environments was overshadowed by the impacts of terrestrially-influenced water masses as the south Florida platform was flooded by rising sea level (Lidz and

Shinn, 1991; Khan et al., 2017). In contrast, the systematic changes in open-ocean ΔR are most likely a reflection of changes in local- to regional-scale ocean circulation during the Holocene.

We hypothesize three potential sources of ^{14}C-depleted water masses to the open-ocean environments of the FKRT, which could have produced the millennial-scale changes in open-ocean ΔR: 1) local upwelling controlled by cyclonic oceanic gyres and meanders of the Florida Current (Lee et al., 1995; Leichter and Miller, 1999), 2) increases in the relative contribution of equatorial water from the South Atlantic to the Western Atlantic (i.e., Kilbourne et al., 2007), and/or 3) changes in the $\Delta^{14}C$ of South Atlantic water masses entering the Caribbean Basin. Below, we first examine the potential for terrestrially-derived sources of elevated nearshore ΔR during the middle Holocene. We then compare the underlying, open-ocean trends in south Florida ΔR throughout the Holocene to regional climatic and oceanographic reconstructions to evaluate the potential sources of open-ocean ΔR variability.

5.1 Drivers of ΔR variability in nearshore environments

The offshore coral reefs of the FKRT occur along the outer margin of Florida's shallow-water continental shelf (Fig. 1c). During the early Holocene, just after the shelf was flooded by rising sea level (~8000 yrs BP; Lidz and Shinn, 1991; Khan et al., 2017), the incipient shelf-edge reefs would have been nearshore environments (Lidz and Shinn, 1991), strongly influenced by the regional hydrology of south Florida. Below, we consider two potential land-based sources of elevated nearshore ΔR during the early to middle Holocene: 1) influx of terrestrially derived sediments associated with the flooding of the south Florida platform, and 2) flow of submarine groundwater onto the reef. Although our nearshore reconstruction of ΔR does include one record from a deeper-water "outlier" reef in Biscayne N.P., which initiated during the early Holocene

(Fowey Rocks, “FR”; see Lidz et al., 2003), most Holocene reefs on the FKRT were established after rising sea-level flooded the shelf margin at ~8000 yrs BP (Lidz and Shinn, 1991; Lidz et al., 2003). We therefore focus our discussion of the potential influence of changes in south Florida hydrology on nearshore ΔR to the period after ~8000 yrs BP and do not attempt to speculate on the drivers of the single ΔR estimate from Biscayne N.P. from the early Holocene.

Florida Bay and Biscayne Bay were formed by rising sea-level and were connected to the Lower Keys, Middle Keys, Upper Keys, and Biscayne N.P. subregions during the middle Holocene, ~6000 years ago (Lidz and Shinn, 1991; Lidz et al., 2003). Flooding of these previously-exposed surfaces could have resulted in significant resuspension of terrestrially derived sediments that would have been transported onto the reefs offshore of the main Florida Keys (Lower, Middle, and Upper Keys) and Biscayne N.P. during the period of elevated nearshore ΔR (Fig. 1c; Fig. 2b; Lidz and Shinn, 1991; Lidz et al., 2003). The coincidence between the putative timing of shelf flooding and elevated nearshore ΔR could suggest that terrestrial sedimentation influenced our nearshore ΔR estimates during this period. Indeed, U-series dating in marine environments is only reliable when the contribution of detrital, non-radiogenic ^{230}Th is insignificant relative to that produced by the ^{238}U→^{234}U→^{230}Th decay chain (Broecker and Thurber, 1965; Cobb et al., 2003; Clark et al., 2014). Terrestrially derived material often contains elevated, detrital (non-radiogenic) ^{230}Th (Clark et al., 2014), even in carbonate systems like the south Florida platform (e.g., Rosenheim et al., 2007); however, elevated non-radiogenic ^{230}Th results in U-series ages that are artificially old (Cobb et al., 2003; Rosenheim et al., 2007), which would produce decreases, not the increases in nearshore ΔR we observed. Furthermore, non-radiogenic ^{230}Th is generally only a significant problem in young carbonates where radiogenic ^{230}Th is low (Cobb et al., 2003; Clark et al., 2014). Because we did not include data that had elevated ^{232}Th and low ^{230}Th/^{232}Th in our models of ΔR (Toth et al., 2017), it is unlikely that increases in nearshore ΔR during the middle Holocene were a result of anomalous U-series ages due to detrital contamination. Instead, we suggest that nearshore ΔR could have been elevated by the influence of ^{14}C-depleted groundwater.

Because of the high permeability of the Pleistocene-aged limestones that form the upper surface of the south Florida platform, groundwater is an important source of hydrologic variability in the region (Cowart et al., 1978; Shinn et al., 1994; Corbett et al., 1999; Reich et al., 2002; Chanton et al., 2003). Florida Bay and southern Biscayne Bay are regions of particularly high transmissivity (Cowart et al., 1978) and, as a result, nearshore locations in Florida Bay, Biscayne Bay, and some inshore areas southeast of the Florida Keys currently experience significant groundwater influence (Shinn et al., 1994; Corbett et al., 1999; Reich et al., 2002; Chanton et al., 2003). Although there is no evidence that groundwater currently reaches the offshore reefs of the FKRT (Böhlke et al., 1999; Corbett et al., 1999; Reich et al., 2006), lower sea level during their early history could have allowed greater groundwater flow to these areas in the past.

As mentioned previously, the shelf-edge reefs of the FKRT would have been shallow-water inshore environments from ~8000–7000 yrs BP, when sea level was ~7–10 m lower than at present (Lidz and Shinn, 1991; Khan et al., 2017). Given that groundwater is currently a significant source of hydrologic variability in inshore areas of the Florida Keys, it is reasonable to assume that groundwater flow on the shelf-edge reefs could have been more important when these reefs were closer to shore. Furthermore, changes in water levels (currently related to tides, storm events, etc.) are known to modulate the pressure gradients that control the flow of groundwater beneath the marine environments of south Florida (Shinn et al., 1994; Reich et al., 2002; Chanton et al., 2003). Thus, lower sea levels during the early part of the Holocene may have increased transmissivity of groundwater through the carbonates of south Florida (Cowart et al., 1978), resulting in more significant groundwater influences during the early development of the FKRT.

As groundwater flows through the limestone of Florida's subterranean aquifers and the upper Pleistocene platform of south Florida, carbonate dissolution and ion exchange can drive significant changes in groundwater geochemistry (Pearson and Hanshaw, 1971; Böhlke et al., 1999; Plummer and Sprinkle, 2001; Dunk et al., 2002; Swarzenski, 2007). The influence of these processes on U-Th disequilibria in groundwater can be complex (Porcelli and Swarzenski, 2003; Swarzenski, 2007). For example, researchers have reported groundwater $^{234}U/^{238}U$ activity ratios that are both higher and lower than modern seawater (1.14–1.15) depending on the conditions under which they formed (Cowart et al., 1978; Dunk et al., 2002; Porcelli and Swarzenski, 2003; Swarzenski, 2007). Little is known about the U-series geochemistry of nearshore groundwater outflows near the FKRT, but there is no evidence of anomalous U-activity in our data (Toth et al., 2017). We also see no evidence of U loss or anomalously high ^{232}Th that would indicate significant changes of U-Th disequilibria in the samples included in our models (Dunk et al., 2002; Porcelli and Swarzenski, 2003; Swarzenski, 2007; Toth et al. 2017). Thus, we assume that the U-series ages of the nearshore corals were not significantly impacted by groundwater contamination; however, more data should be collected on the radiochemistry of groundwater in this region to test this hypothesis.

In contrast, contributions of ^{14}C-depleted carbonates can have substantial impacts on radiocarbon ages. As a result the "hard water effects" associated with the interactions of water masses with old carbonates, groundwater is generally significantly depleted in ^{14}C relative to the open ocean (Pearson and Hanshaw, 1971; Böhlke et al., 1999; Plummer and Sprinkle, 2001). The influence of ^{14}C-depleted carbonates is most significant in Florida's deep aquifers (Pearson and Hanshaw, 1971; Plummer and Sprinkle, 2001); however, even groundwater that accumulated recently in the Pleistocene-aged carbonates of Florida Bay has been shown to have anomalously low ^{14}C (Böhlke et al., 1999).

A more significant influx of ^{14}C-depleted groundwater during the middle Holocene could explain the increases in nearshore ΔR we observed from ~8000–6600 yrs BP. By ~5000 yrs BP, when nearshore ΔR had decreased to values more similar that of the open ocean, sea level would have been just ~3.5 m below its present position (Khan et al., 2017) and the nearshore reefs of the FKRT would have been located at least 3–5 km offshore (Lidz and Shinn, 1991). Furthermore, the modern hydrologic regime of south Florida was established by ~4000 yrs BP, as the Florida Bay and Biscayne Bay and the tidal passages connecting the Bays to the Atlantic would have been flooded by rising sea level by this time (Lidz and Shinn, 1991; Lidz et al., 2007). Together, these changes would suggest that by ~4000 yrs BP, when nearshore ΔR was similar to that of the open ocean, groundwater influence on the shelf-edge reefs of Biscayne N.P. and the Keys subregions was minimal, as it is today (Böhlke et al., 1999; Corbett et al., 1999; Reich et al., 2006).

5.2 Local upwelling and open-ocean ΔR

To evaluate the hypothesis that variability in the frequency or intensity of local upwelling could have been responsible for the millennial-scale changes in open-ocean ΔR on the FKRT, we compare our reconstruction of ΔR to three previously-published paleoceanographic records of the planktonic foraminifera, *Globigerinoides ruber*, from cores collected from the southwestern

Straits of Florida (Fig. 3): 1) a record of *G. ruber* $\delta^{18}O_{calcite}$, which varies as a function of relative sea-surface temperature (SST) and sea surface salinity (SSS), from the middle Holocene (~5000 yrs BP) to present (Fig. 3b; Lund and Curry, 2004); 2) a SST reconstruction from the early to middle Holocene (~9000–6000 yrs BP) from *G. ruber* Mg/Ca (Fig. 3c; Schmidt et al., 2012); and 3) an inferred relative SSS record (based on $\delta^{18}O_{sw}$) for the same period during the early Holocene derived from paired measurements of *G. ruber* Mg/Ca and $\delta^{18}O_{calcite}$ (Fig. 3d; Schmidt et al., 2012). We produced new age models for the records after recalibrating the data with latest marine calibration curve (Marine 13; Reimer et al., 2013) using the R program Bacon (Blaauw and Christen, 2011). Our models of ΔR were parameterized to reconstruct millennial-scale variability (i.e., the hyperparameter for temporal scale of the model optimized at 850 years). We therefore smoothed the published datasets using a 1000-yr running mean to standardize the temporal resolution of these records and to make them more directly comparable to our models. The core records were collected ~40 km offshore of the Dry Tortugas N.P. (Lund and Curry, 2004; Lynch-Stieglitz et al., 2009; Schmidt et al., 2012) where our open-ocean records were collected and should, therefore, be representative of the general changes in the hydrographic variability of surface waters in this region. Unfortunately, similar paleoceanographic records do not exist for the rest of the FKRT, so we cannot evaluate the impact of local upwelling on the nearshore sites; however, because upwelling is driven by similar processes throughout the region (i.e., meanders of the Florida Current) we assume that the nearshore sites would have experienced similar variability in local oceanography throughout their Holocene history.

Although there appear to be some broad correlations between the foraminiferal records from the Straits of Florida and the millennial-scale changes in open-ocean ΔR, closer consideration of the records suggests that local upwelling was not the cause of ΔR variability in this region. A regime of more intense upwelling along the Florida reef tract should result in regional cooling of shallow-water sea temperatures along the northern boundary of the Florida Straits (Lee et al., 1995; Leichter and Miller, 1999). Additionally, although Lee et al. (1995) suggested that upwelled waters within the Tortugas Gyre were relatively fresh, water-column profiles from throughout the FKRT have demonstrated that intermediate water (>250 m depth) sources are high in salinity relative to the surface (Leichter et al., 2007). Thus, upwelling should also drive increases in regional SSS. Conversely, increases in open-ocean ΔR in our record are generally associated with increases in SST and/or decreases in SSS ($\delta^{18}O_{sw}$) in the records from the Straits of Florida (Fig. 3), which is the opposite of what would be expected if local upwelling were driving the variability in ΔR on the FKRT. Furthermore, records from the northern Gulf of Mexico suggest a strong Loop Current during the middle Holocene (Poore et al., 2003), which has been suggested to produce more frequent formation of Tortugas Gyres (Lee et al., 1995) and thus upwelling, but ΔR was lowest at this time.

Overall, the available data support Schmidt et al.'s (2012) conclusion that upwelling associated with the Tortugas Gyre was not a significant driver of the variability in sea-surface conditions in the Straits of Florida during the Holocene. Instead, we conclude that despite the influence of periodic upwelling, the regional shallow-water environments are relatively well-stratified over millennial timescales (Druffel et al., 2008). A minimal influence of local mixing on the FKRT is supported by the generally negative values of open-ocean ΔR (averaging -60±33 years over the last 8,000 years and -64±27 years at present; Table 2; Fig. 2) and implies that broader-scale oceanographic changes were likely responsible for the observed variability in ΔR during the Holocene.

We note, however, that the modern estimates of ΔR from the FKRT reported in Reimer and Reimer's (2001) Marine Radiocarbon Database (http://calib.qub.ac.uk/marine/) are significantly higher than our modeled present-day values (open-ocean: -64±27; nearshore: -54±32). Reimer and Reimer's (2001) estimate of modern ΔR based on Lighty et al.'s (1982) ^{14}C age of a coral collected from Dry Tortugas N.P. in 1884 was 114±51. Similarly, the weighted average of five modern estimates of ΔR from the Upper Keys was 3±13 (Druffel and Linick, 1978; Druffel, 1997a; Reimer and Reimer, 2001). Although Druffel and Linick's [1978] and Druffel's [1997] modern ΔR values are all within error of our modern estimate when considered individually, it is possible that our modeled values underestimate modern ΔR in the region. Higher modern-day ΔR would suggest that local upwelling may play a more significant role at present than it did in the past, but more measurements of modern radiocarbon variability are needed to test this hypothesis.

5.2 Western Atlantic circulation and open-ocean ΔR

The similarity between our modern estimates of ΔR and published records of modern ΔR from shallow-water environments throughout the Western Atlantic (Table 2; Marine Reservoir Database [Reimer and Reimer, 2001]) supports the conclusion that the surface waters of the tropical and sub-tropical Western Atlantic are well-mixed (Wagner et al., 2009; Kilbourne et al., 2007). We hypothesize, therefore, that radiocarbon variability in the surface water around the Straits of Florida may reflect changes in the sources or properties of water masses to the Caribbean Basin as a whole (Kilbourne et al. 2007), rather than the influence of local oceanographic processes (c.f., Guilderson et al., 2004; Kilbourne et al., 2007).

Surface waters enter the Caribbean Basin through a variety of passages along the Antilles island chain (Fig. 1b; Schmitz and Richardson, 1991; Wilson and Johns, 1997; Johns et al., 2002). These waters converge to form the westward flowing Caribbean Current, which continues into the Gulf of Mexico as the Yucatan Current, and ultimately exit the region via the Florida Current in the Straits of Florida (Fig. 1b; Schmitz and Richardson, 1991; Johns et al., 2002). Johns et al. (2002) demonstrated that the total inflow of surface waters into the Caribbean, ~28 Sverdrups (Sv), is divided almost equally between three major passages along the island chain (see also Schmitz and Richardson, 1991): the Greater Antilles passages in the north (~10 Sv), the northern portion of the Lesser Antilles, known as the Leeward Islands (~8 Sv), and the southern Lesser Antilles, known as the Windward Islands (~10 Sv); however, whereas the inflow of water through the southern, Windward Islands of the Lesser Antilles is dominantly sourced from the South Atlantic, inflow through the Leeward Islands of the Lesser Antilles and the Greater Antilles is driven by the westward flow of the North Atlantic subtropical gyre (Fig. 1a,b; Schmitz and Richardson, 1991; Wilson and Johns, 1997; Johns et al., 2002).

The inflow through the southern, Windward Passage of the Lesser Antilles is of particular interest in interpreting regional changes in open-ocean ΔR because the equatorial water masses from the South Atlantic (Fig. 1a) are relatively depleted in ^{14}C as a result of upwelling off the western coast of Africa (Southon et al., 2002; Key et al., 2004; Kilbourne et al., 2007; Lewis et al., 2008; Dewar et al., 2012). In contrast, in the North Atlantic subtropical gyre (Fig. 1a), ^{14}C is high because intense northeast trade winds and long residence times promote active gas exchange between surface waters and the atmosphere (Broecker et al., 1960; Key et al., 2004; Kilbourne et al., 2007). Millennial-scale shifts in Caribbean source water should, therefore, be reflected as changes in open-ocean ΔR during the Holocene.

At present, the ^{14}C-depleted water masses of the equatorial South Atlantic are putatively the dominant source of surface waters to the region (Kilbourne et al., 2007), but the relative contribution of equatorial and subtropical waters can vary over interannual to decadal timescales (Johns et al., 2002; Kilbourne et al., 2007). One potential driver of time-varying Caribbean source water is changes in large-scale patterns of Atlantic circulation associated with the strength of AMOC. The proportion of equatorial South Atlantic water entering the Caribbean should be related to the strength of AMOC because deepwater production in the North Atlantic (Fig. 1a) must be balanced by the northward transport of surface waters from the South Atlantic (Broecker, 1991; Schmitz and Richardson, 1991; Schmitz and McCartney, 1993; Johns et al., 2002; Kilbourne et al., 2007). Thus, periods of stronger AMOC should increase the relative contribution of equatorial water masses to the Caribbean whereas subtropical, North Atlantic sources should dominate during periods of weaker AMOC (Wilson and Johns, 1997; Johns et al., 2002; Kilbourne et al., 2007).

It is well-established that the intensity of AMOC was highly sensitive to climate variability across glacial-to-interglacial cycles (Broecker, 1991; Clark et al., 2002). In contrast, the variability in AMOC and its climatic correlates during the relatively mild climate of the Holocene are not as well-constrained (Thornalley et al., 2009, 2013). The most recent records of North-Atlantic Deep Water (NADW) formation from the Nordic Sea of the Northern Atlantic (Fig. 1a) suggest that AMOC was relatively weak during the early and late Holocene and strongest during the middle Holocene thermal maximum ~7000 yrs BP (Thornalley et al., 2009, 2013), which is the opposite of what we would predict based on the records of open-ocean ΔR from the FKRT (Fig. 2a); however, model simulations suggest that climatic and oceanographic forcing within the Labrador Sea, the other site of NADW formation (Fig. 1a; Schmitz and

McCartney, 1993; Lumpkin and Speer, 2003), was a central driver of AMOC variability during the Holocene (Schultz et al., 2007). Records from this region of the North Atlantic are not as well-resolved, but some reconstructions suggest somewhat opposing changes compared with the Nordic Sea, with increased formation of NADW before and after ~7000 yrs BP (e.g., Solignac et al., 2004; Schultz et al., 2007). These trends are more consistent with the relatively high ΔR throughout the FKRT during the early Holocene and at ~3000 yrs BP and the low open-ocean ΔR at ~7000 yrs BP (Fig. 2a).

We also consider the possibility that AMOC variability was not the only driver of time-varying contributions of South Atlantic water to the Caribbean. Indeed, the relative proportion of equatorial versus subtropical waters entering the Caribbean necessarily depends not only on the strength of South Atlantic inflow through the Windward Passages of the Lesser Antilles, but also the strength of inflow from the subtropical gyre through the northern passages (Fig. 1a; Johns et al., 2002). All else being equal, decreases in the strength of subtropical gyre circulation should increase the inflow of waters from the South Atlantic to the Caribbean. Kim et al. (2007) produced a multi-proxy record of subtropical gyre circulation during the Holocene from alkenone-based records of SST and oceanic productivity along the northwest coast of Africa, the location of the Canary Current (Fig. 1a), which forms the eastern arm of the gyre. Their reconstruction suggests that subtropical gyre circulation was strongest from ~7500–3500 yrs BP and after ~1500 yrs BP, and relatively weak during other periods of the Holocene (Kim et al., 2007). Assuming that strong subtropical gyre circulation should result in reduced contributions of ^{14}C-depleted South Atlantic water to the Caribbean, and that a weak subtropical gyre would increase the inflow of South Atlantic water, Kim et al.'s (2007) reconstruction is consistent with the hypothesis that varying influence of North Atlantic waters contributed to the variability in open-ocean ΔR on the FKRT (Fig. 2a). Although a more comprehensive understanding of broad-scale changes in Atlantic circulation is needed to definitely link variability in the strength of both North Atlantic subtropical gyre and AMOC to radiocarbon variability, we suggest that millennial-scale changes in the relative contributions of South Atlantic and North Atlantic source waters could have been important driver of millennial-scale changes in open-ocean ΔR on the FKRT.

Assuming that the radiocarbon variability of the Caribbean, and by extension the FKRT, is controlled primarily by the supply of ^{14}C-depleted surface water from the equatorial South Atlantic, then changes in the Δ^{14}C of South Atlantic waters due to variability in west African upwelling could also have a significant impact on variability in open-ocean ΔR on the FKRT. Paleoceanographic reconstructions suggest that the coastal upwelling systems associated with the Canary and Benguela Currents (Fig. 1a) in this region have experienced significant millennial-scale variability in upwelling intensity (e.g., deMenocal et al., 2000; Kim et al., 2003; Kim et al., 2007). The records from the northwest African coast associated with Canary Current upwelling are generally out of phase with the variations in open-ocean ΔR observed on the FKRT (Fig. 2a; deMenocal et al., 2000; Kim et al., 2007); however, it is possible that the signature ^{14}C-depleted water from this region is diluted because the upwelled waters of the Canary Current mix with the ^{14}C-enriched waters of the subtropical gyre (Schmitz and McCartney, 1993; Kilbourne et al., 2007; Kim et al., 2007). The strongest signature of western African upwelling on Caribbean inflow should originate from the Benguela upwelling system to the south (Fig. 1a), where ΔR is significantly elevated (Southon et al., 2002; Dewar et al., 2012). Paleoceanographic reconstructions of upwelling intensity from this region based on latitudinal SST gradients derived from alkenones (Kim et al., 2003), relative estimates of SST based on the abundance of cysts from the dinoflagellate, *Polyshaeridium zoharyi* (Shi et al., 2000), and a record of the strength of the SE trade winds based on abundance of the coccolithophore, *Florisphaera profunda* (McIntyre and Molfino, 1996) all support the conclusion that Benguelan upwelling peaked during the early Holocene and around ~3000 yrs BP, when ΔR throughout the FKRT was high (Fig. 2a), and suggest that upwelling was weak ~7000 yrs BP, when open-ocean ΔR on the FKRT was lowest (Fig. 2a). Stronger Benguelan upwelling around 3000 yrs BP is also supported by a record of ΔR from southern Africa (Dewar et al., 2012). We hypothesize that the millennial-scale variability we observed in ΔR on the FKRT resulted from a combination of shifts in the relative contribution of South Atlantic water to the region and changes in the $\Delta^{14}C$ of that water related to millennial-scale changes in the intensity of the Benguela upwelling system off western Africa. As a first-order test of this hypothesis, future studies could use data on the modern $\Delta^{14}C$ of potential source waters to evaluate the magnitude of changes in south Atlantic $\Delta^{14}C$ that would be needed to produce the observed changes in south Florida ΔR; however, additional reconstructions of millennial-scale radiocarbon variability from throughout the western Atlantic are needed to fully resolve its paleoceanographic drivers.

5.3 Implications for ^{14}C dating

The significant millennial-scale changes in ΔR on the FKRT have important implications for the accuracy of radiocarbon ages from marine samples in this region. Whereas the magnitude of modern ΔR has been quantified in some locations in the western Atlantic, few studies have attempted to quantify the variability in surface-water ^{14}C through time, and ours are the only records from the western Atlantic that span the entire Holocene (Reimer and Reimer, 2001). As a result, researchers generally rely on a single, modern estimate of ΔR from a region to calibrate marine samples, and assume that ΔR does not vary through time (Stuiver et al., 1986; Reimer and Reimer, 2001). Although the magnitude of millennial-scale variability in ΔR we observed was less extreme than in regions that directly experience strong upwelling (e.g., coastal upwelling along western continental boundaries [Ingram, 1998; Fontugne et al. 2004], wind-driven upwelling systems [Toth et al. 2015], and equatorial systems [Zaunbrecher et al. 2010]), our study demonstrates that the assumption of a stationary ΔR should be re-evaluated, even in oceanographically benign regions such as the western Atlantic.

As an example of the potential errors associated with using inaccurate estimate of ΔR, we calibrated the conventional ^{14}C age of a middle Holocene coral from Dry Tortugas N.P.—5960±35 (DT-GB-7-27)—using a ΔR based on 1) a living coral colony from the Dry Tortugas N.P. (ΔR=114±51; Lighty et al., 1982), 2) living corals from the Upper Keys (ΔR=3±13; Druffel and Linick, 1978; Druffel, 1997a), 3) a weighted mean of those two values (ΔR=8±29; Reimer and Reimer 2001), 4) the modern open-ocean value from our model (ΔR=-64±27), and 5) the age-specific open-ocean model prediction for the conventional ^{14}C age of the coral (ΔR=-104±25). The "true" ^{230}Th age of the coral is 6096±23 years.

The results of each calibration are presented in Figure 4. The modern estimates of ΔR for the FKRT from previous studies currently available in the Marine Reservoir Database (ΔR 1–3; Reimer and Reimer, 2001) all result in calibrated ^{14}C ages that are significantly younger than the true age of the sample. The 2σ range of the calibrated age based on our estimate of modern open-ocean ΔR does overlap with the true age of the sample, but the median of the calibration (yrs BP) is ~60 years too young. Although these errors may seem minor, high precision ages are critical when they are used in age-based calculations such as sedimentation or accretion rates. Only the age-specific estimate of open-ocean ΔR from our model provides a median age estimate that approximates the true age of the sample.

Although it may not always be possible, quantifying the regional temporal variability in ΔR can significantly improve the accuracy and precision of radiocarbon dating. Using our statistical models of ΔR versus conventional ^{14}C age, we provide a database of predicted ΔR values and associated 1σ uncertainties for open-ocean and nearshore environments of south Florida. These data are available at https://doi.org/10.5066/F7P8492Q. Our model outputs parallel the resolution of the marine calibration curve, providing age-specific estimates of ΔR±1σ at 5-year intervals over the Holocene. In order to provide the most accurate calibrated age estimates, our models can and should be applied to any new Holocene radiocarbon ages of marine samples collected from the region. Whereas the nearshore model should be used for coastal areas from the Lower Keys through southeast Florida, we suggest that the open-ocean model can be applied to calibrations from any offshore locations in south Florida

6. Conclusions

We report the first millennial-scale models of radiocarbon variability for the western Atlantic. Our reconstruction demonstrates that there was significant spatial and temporal variability in the ΔR of the FKRT over millennial timescales. This variability has important implications not only for the accuracy of radiocarbon dating in this region, but also for our understanding of local- to regional-scale changes in hydrology and oceanic circulation during the Holocene. We suggest that whereas the nearshore environments of the Florida Keys and Biscayne N.P. were influenced by relatively higher groundwater influx during the middle Holocene (driving nearshore ΔR higher), ΔR variability in the open-ocean environments of Dry Tortugas N.P. and the Marquesas reflect broad-scale changes in Atlantic circulation. Comparison of our record of open-ocean ΔR to existing paleoceanographic reconstructions from south Florida suggests that local upwelling was not an important driver of millennial-scale open-ocean

ΔR variability in south Florida. Instead, our record supports the hypothesis that open-ocean radiocarbon variability in the Caribbean, and by extension, the FKRT resulted from changes in the character and relative contribution of South Atlantic source water to the region. Our results add to a growing body of research that highlights the value of reconstructions from the marine environments of south Florida to our understanding of climatic and oceanographic oscillations over a broad spatial scale.

Acknowledgements

We thank the following researchers whose work in the Florida Keys provided many of the core records used in this study: Eugene Shinn, Harold Hudson, Robert Halley, Barbara Lidz, Daniel Robbin, Christopher Reich, T. Don Hickey, H. Gray Multer, J. Edward Hoffmeister, Marguerite Toscano, and Joyce Lundberg. These previously collected cores sampled from the USGS Core Archive (http://olga.er.usgs.gov/coreviewer/) were collected under permits from Dry Tortugas National Park (formerly Fort Jefferson National Monument), Biscayne National Park (formerly Biscayne National Monument), the Florida Keys National Marine Sanctuary (FKNMS), and the Florida State Department of Natural Resources. New cores from the Upper and Middle Keys were collected under permit numbers FKNMS-2013-097-A1 and FKNMS-2015-054, repectively by L.T.T., Anestasios Stathakopoulos, B.J. Reynolds, Hunter Wilcox, Jennifer Morrison, and Marc Blouin of the USGS. We thank Jack McGeehin of the USGS Radiocarbon Dating Laboratory for facilitating the radiocarbon analysis for this study. XRD analyses of the corals were conducted as part of USGS studies led by C. Reich and H.D. Hickey and J. Flannery of the USGS assisted with SEM-imaging of the samples. Daniel R. Muhs and N.S. Khan of the USGS provided helpful commentary on early drafts of the manuscript. This study was supported by a Mendenhall Research Fellowship awarded to L.T.T. by the United

States Geological Survey (USGS) Coastal and Marine Geology Program and the Natural Hazards Mission Area, and by the Climate and Land Use Research and Development Program of USGS. Erica Ashe was supported by U.S. National Science Foundation [grant numbers ARC-1203415, OCE-1458904], National Oceanic and Atmospheric Administration [grant number NA11OAR431010], and the New Jersey Sea Grant Consortium. All data used in this manuscript are published and freely available for download in USGS data release at https://doi.org/10.5066/F7P8492Q. Any use of trade, firm, or product names is for descriptive purposes only and does not imply endorsement by the United States Government.

References

Blaauw M., Christen, A.J., 2011. Flexible Paleoclimate Age-Depth Models Using an Autoregressive Gamma Process. Bayesian Analysis, 6, 457–474.

Böhlke, J.K., Plummer, L.N., Busenberg, E., Coplen, T.B., Shinn, E.A., Schlosser, P., 1999. Origins, residence times, and nutrient sources of marine ground water beneath the Florida Keys and nearby offshore areas. U.S. Geological Survey Program on the South Florida Ecosystem, Open-File Report 99–181, 2–3.

Brock, J.C., Palaseanu-Lovejoy, M., Poore, R.Z., Nayegandhi, A., Wright, C.W., 2010. Holocene aggradation of the Dry Tortugas coral reef ecosystem. Coral Reefs 29, 857–868.

Broecker, W.S., 1991. The great ocean conveyor. Oceanography 4, 79–89.

Broecker W.S., Olson, E.A., 1961. Lamont Radiocarbon Measurements VIII. Radiocarbon 3, 176–204.

Broecker, W.S., Gerard, R., Ewing, M., Heezen, B.C., 1960, Natural radiocarbon in the Atlantic Ocean, J. Geophys. Res. 65, 2903–2931.

Broecker, W.S., Thurber, D.L., 1965, Uranium-series dating of corals and oolites from Bahaman and Florida Key Limestones. Science 149, 58–60.

Came, R.E., Oppo, D.W., Curry, W.B., Lynch-Stieglitz, J., 2008. Deglacial variability in the surface return flow of the Atlantic meridional overturning circulation. Paleoceanography 23, PA001450.

Chanton, J.P., Burnett, W.C., Dulaiova, H., Corbett, D.R., Taniguchi, M., 2003. Seepage rate variability in Florida Bay driven by Atlantic tidal height 66, 187–202.

Cheng H., Edwards, R.L., Shen, C.-C., Polyak, V.J., Asmerom, Y., Woodhead, J., Hellstrom, J., Wang, Y., Kong, X., Spötl, C., Wang, X., Alexander, E.C., 2013. Improvements in Th-230 dating, Th-230 and U-234 half-life values, and U-Th isotopic measurements by multicollector inductively coupled plasma mass spectrometry. Earth Planet. Sci. Lett. 371, 82–91.

Clark, P.U., Pisias, N.G., Stocker, T.F., Weaver, A.J., 2002. The role of thermohaline circulation in abrupt climate change. Nature 415, 863–869.

Clark, T.R., Roff, G., Zhao, J.-x., Feng, Y.-x., Done, T.J., Pandolfi, J.M., 2014. Testing the precision and accuracy of the U–Th chronometer for dating coral mortality events in the last 100 years. Quat. Geochron. 23, 35–45.

Cobb K.M., Charles, C.D., Cheng, H., Kastner, M., Edwards, R.L., 2003. U/Th-dating living and young fossil coral from the central tropical Pacific. Earth and Planetary Science Letters 210, 91–103.

Corbett, D.R., Chanton, J., Burnett, W., Dillon, K., Rutkowski, C., Fourqurean, J.W., 1999. Patterns of groundwater discharge into Florida Bay. Limnol. Oceanogr. 44, 1045–1055.

Cowart, J.B., Kaufman, M.I., Osmond, J.K., 1978. Uranium-isotope variations in groundwters of the Floridian aquifer and Boulder Zone of south Florida. J. Hydrol. 36, 161–172.

Cross, T.S., Cross, B.W., 1983. U, Sr, and Mg in Holocene and Pleistocene corals *A. palmata* and *M. annularis*. J. Sed. Petrol. 53, 587–594.

Davis, K.A., Leichter, J.J., Hench, J.L., Monismith, S.G., 2008. Effects of western boundary current dynamics on the internal wave field of the southeast Florida shelf. J. Geophys. Res. 113, C09010.

DeMenocal, P., Ortiz, J., Guilderson, T., Sarnthein, M., 2000. Coherent high- and low-latitude climate variability during the Holocene warm period. Science 288, 2198–2202.

Dewar, G., Reimer, P.J., Sealy, J., Woodborne, S., 2012. Late-Holocene marine radiocarbon reservoir corretion (ΔR) for the west coast of South Africa. The Holocene 22, 1481–1489.

Druffel, E.M., Linick, T.W., 1978. Radiocarbon in annual rings of Florida. Geophys. Res. Lett. 5, 913–916.

Druffel, E.M., 1997a. Pulses of rapid ventilation in the north Atlantic surface ocean during the past century. Science 275, 1454–1457.

Druffel, E.R.M. 1997b. Geochemistry of corals: Proxies of past ocean chemistry, ocean circulation, and climate. Proc. Nat. Acad. Sci., USA, 94, 8354–8361.

Druffel, E.R.M., Robinson, L.F., Griffin, S., Halley, R.B., Southon, J.R., Adkins, J.F., 2008. Low reservoir ages for the surface ocean from mid-Holocene Florida corals. Paleoceanography 23, PA2209.

Dunk, R.M., Mills, R.A., Jenkins, W.J., 2002. A reevaluation of the oceanic uranium budget for the Holocene. Chem. Geol. 190, 45–67.

Fontugne, M., Carré, M., Bentaleb, I., Julien, M., Lavallée, D., 2004. Radiocarbon reservoir age variations in the South Peruvian upwelling during the Holocene. Radiocarbon 46, 531–537.

Ginsburg, R.N., Shinn, E.A., 1994. Preferential distribution of reefs in the Florida Reef Tract: the past is the key to the present. Pages 21–26 in Colloquium on global aspects of coral reefs: health, hazards, and history, Rosenstiel School of Marine and Atmospheric Science, University of Miami, Florida.

Guilderson, T.P., Cole, J.E., Southon, J.R., 2004. Pre-bomb $\Delta^{14}C$ variability and the Suess Effect in Cariaco Basin Surface Waters as Recorded in Hermatypic Corals. Radiocarbon 47, 57–65.

Gyory, J., Rowe, E., Mariano, A.J., Ryan, E.H., 2013. Ocean Surface Currents. http://oceancurrents.rsmas.miami.edu/caribbean.html.

Hall, M.M., Bryden, H.L., 1982, Direct estimates and mechanisms of ocean heat transport. Deep-Sea res. 29, 339–359.

Ingram, B.L., 1998. Differences in radiocarbon age between shell and charcoal from a Holocene shellmound in northern California. Quat. Res. 49:102–110.

Johns, W.E., Townsend, T.L., Fratantoni, D.M., Wilson, W.D., 2002. On the Atlantic inflow to the Caribbean Sea. Deep-Sea Res. Part I 49, 211–243.

Khan, N.S., Ashe, E. Horton, B.P., Dutton, A., Kopp, R.E., Brocard, G., Engelhart, S., Hill, D.F., Peltier, W.R., Vane, C.H., Scatena, F.N., 2017, Drivers of Holocene sea-level change in the Caribbean. Quat. Sci. Rev. 155, 13–36.

Key, R.M., Kozyr, A., Sabine, C.L., Lee, K., Wanninkhof, R., Bullister, J.L., Feeley, R.A., Millero, F.J., Mordy, C., Peng, T.-H., 2004. A global ocean carbon climatology: results from Global Data Analysis Project (GLODAP). Glob. Biogeochem. Cycles 18, GB4301.

Kilbourne, K.H., Quinn, T.M., Guilderson, T.P., Webb, R.S., Taylor, F.W., 2007. Decadal- to interannual-scale source water variations in the Caribbean Sea recorded by Puerto Rican coral radiocarbon. Clim. Dyn. 29, 51–62.

Kim, J.-H., Schneider, R.R., Mulitza, S., Müller, P.J., 2003. Reconstruction of SE trade-wind intensity based on sea-surface temperature gradients in the Southeast Atlantic over the last 25 kyr. Geophys. Res. Lett. 30, GL017557.

Kim, J.-H., Meggers, H., Rimbu, N., Lohmann, G., Freudenthal, T., Müller, P.J., Schneider, R.R., 2007. Impacts of the North Atlantic gyre circulation on Holocene climate off northwest Africa. Geology 35, 387–390.

Klein, C.J., Orlando, S.P., 1994. A spatial framework for water-quality management in the Florida Keys National Marine Sanctuary. Bull. Mar. Sci. 54, 1036–1044.

Key, R.M., Kozyr, A., Sabine, C.L., Lee, K., Wanninkhof, R., Bullister, J.L., Feely, R.A., Millero, F.J., Mordy, C., Peng, T.-H., 2004. A global ocean carbon climatology: results from Global Data Analysis Project (GLODAP). Glob. Biogeochem. Cycles 18, GB4031.

Kopp, R.E., Kemp, A.C., Bittermann, K., Horton, B.P., Donnelly, J.P., Gehrels, W.R., Hay, C.C., Mitrovica, J.X., Morrow, E.D., Rehmstorf, S., 2016. Temperature-driven global sea-level variability in the Common Era. Proc. Natl. Acad. Sci. USA 113, E1434–E1441.

Lee, T.N., Leaman, K., Williams, E., Berger, T., Atkinson, L., 1995. Florida Current meanders and gyre formation in the southern Straits of Florida. J. Geophys. Res. 100, 8607–8620.

Leichter, J.J., Miller, S.L., 1999. Predicting high-frequency upwelling: spatial and temporal patterns of temperature anomalies on a Florida coral reef. Cont. Shelf Res. 19, 911–928.

Leichter, J.J., Paytan, A., Wankel, S., Hanson, K., Miller, S., Altabet, M.A., 2007. Nitrogen and oxygen isotopic signatures of subsurface nitrate seaward of the Florida Keys reef tract. Limnol. Oceanogr. 52, 1258–1267.

Lewis, C.A., Reimer, P.J., Reimer, R.W., 2008. Marine reservoir corrections: St. Helena, south Atlantic ocean. Radiocarbon 50, 275–280.

Lidz, B.H., Shinn, E.A., 1991. Paleoshorelines, reefs, and a rising sea: south Florida, U.S.A. J. Coast. Res. 7, 203–229.

Lidz, B.H., Reich, C.D., Shinn, E.A., 2003. Regional Quaternary submarine geomorphology in the Florida Keys. Geol. Soc. Am. Bull. 115, 845–866.

Lighty, R.G., Macintyre, I.G., Stuckenrath, R., 1982. *Acropora palmata* reef framework: a reliable indicator of sea level in the western Atlantic for the past 10,000 years. Coral Reefs 1, 125–130.

Lumpkin, R., Speer, K., 2003. Large-scale vertical and horizontal circulation in the North Atlantic Ocean. J. Phys. Ocean. 33, 1902–1920.

Lund, D.C., Curry, W.B., 2004. Late Holocene variability in Florida Current surface density: patterns and possible causes. Paleoceanography 19, PA4001.

Lund D.C., Curry, W., 2006. Florida Current surface temperature and salinity variability during the last millennium. Paleoceanography 21, PA2009.

Lynch-Stieglitz, J., Curry, W.B., Slowey, N., 1999. Weaker Gulf Stream in the Florida Straits during the Last Glacial Maximum. Nature 402, 644–648.

Lynch-Stieglitz, J., Curry, W.B., Lund, D.C., 2009. Florida straits density structure and transport over the last 8000 years. Paleoceanography 24, PA3209.

McHutchon, A., Rasmussen, C.E., 2011. Gaussian process training with input noise. Advances in Neural Information Processing Systems, 1341–1349.

McIntyre, A., Molfino, B., 1996. Forcing of Atlantic equatorial and subpolar millennial cycles by precession. Science 274, 1867–1870. Hydrogeol. J. 9, 127–150.

Muhs, D.R., Simmons, K.R., Schumann, R.R., Halley, R.B., 2011. Sea-level history of the past two interglacial periods: new evidence from U-series dating of reef coral from south Florida. Quaternary Science Reviews 30, 570–590.

Pearson, F.J., Hanshaw, B.B., 1971. Sources of dissolved carbonate species in groundwater and their effects on carbon-14 dating. Proceedings of a Symposium on Use of Isotopes in Hydrology, International Atomic Energy Agency, 271–286.

Plummer, L.N., and Sprinkle, C.L., 2001, Radiocarbon dating of dissolved inorganic carbon in groundwater from confined parts of the upper Floridian aquifer, Florida, USA. Hydrogeol. J. 9, 127–150.

Poore, R.A., Dowsett, H.J., Verardo, S., Quinn, T.M., 2003. Millennial- to century-scale variability in the Gulf of Mexico Holocene climate records. Paleoceanography 18, PA1048.

Porcelli, D., Swarzenski, P.W., 2003, The behavior of U- and Th-series nuclides in groundwater, Reviews in Mineralogy and Geochemistry 52, 317–361.

Precht, W.F., Miller, S.L., 2007. Ecological shifts along the Florida reef Tract—The past as a key to the future, in Aronson, R.B., ed., Geological approaches to coral reef ecology: New York, Springer Science+Business Media, LLC., 237–312.

R Core Team, 2014. R: A language and environment for statistical computing. R Foundation for Statistical Computing, Vienna, Austria. http://www.R-project.org/.

Rasmussen, C.E., Williams, C.K.I., 2006. Guassian processes for machine learning. The MIT Press, Caimbridge.

Reich, C.D., Shinn., E.A., Hickey, T.D., Tihansky, A.B., 2002. Tidal and meteorological influences on shallow marine groundwater flow in the Upper Florida Keys. In Porter, J.W., Porter, K.G., The Everglades, Florida Bay, and Coral Reefs of the Florida Keys An Ecosystem Sourcebook. CRC Press, Boca Raton, FL, p. 659–676.

Reich, C.D., Halley, R.B., Hickey, T., Swarzenski, P., 2006. Groundwater characterization and assessment of contaminants in marine areas of Biscayne National Park. National Parks Service Technical Report NPS/NRWRD/NRTR-2006/356.

Reich, C.D., Hickey, T.D., DeLong, K.L., Poore, R.Z., Brock, J.C., 2009. Holocene core logs and site statistics for modern patch-reef cores: Biscayne National Park, Florida. U.S. Geological Survey Open-File Report 2009–1246.

Reich, C.D., Streuebert, M., Dwyer, B., Godbout, M., Muslic, A., Umberger, D., 2012. St. Petersburg Coastal and Marine Science Center's core archive portal. USGS Data Series 626. http://pubs.usgs.gov/ds/626/.

Reimer, P.J., Reimer, R.W., 2001. A marine reservoir correction database and on-line interface. Radiocarbon 43, 461–463.

Reimer, P.J., Bard, E., Bayliss, A., Beck, J.W., Blackwell, P.G., Ramsey, C.B., Buck, C.E., Cheng, H., Edwards, R.L., Friedrich, M., Grootes, P.M., Guilderson, T.P., Haflidason, H., Hajdas, I., Hatté, C., Heaton, T.J., Hoffmann, D.L., Hogg, A.G., Hughen, K.A., Kaiser, K.F., Kromer, B., Manning, S.W., Niu, M., Reimer, R.W., Richards, D.A., Scott, E.M., Southon, J.R., Staff, R.A., Turney, C.S.M., van der Plicht, J., 2013. IntCal13 and Marine13 radiocarbon age calibration curves 0–50,000 years yrs BP. Radiocarbon 55, 1869–1887.

Rosenheim, B.E., Swart, P.K., Eisenhauer, A., 2007. Constraining initial ^{230}Th activity in incrementally deposited, biogenic aragonite from the Bahamas. Geochim. Cosmochim. Acta 71, 4025–4035.

Schmidt, M.W., Weinlein, W.A., Marcantonio, F., Lynch-Stieglitz, J., 2012. Solar forcing of Florida Straits surface salinity during the early Holocene. Paleoceanography 27, PA3204.

Schmitz, W.J., Richardson, P.L., 1991, On the sources of the Florida Current. Deep-Sea Res. 38, S379–S409.

Schmitz, W.J., McCartney, M.S., 1993, On the north Atlantic circulation. Rev. Geophys. 31, 29–49.

Schultz, M., Prange, M., and Klocker, A., 2007, Low-frequency oscillations of the Atlantic Ocean meridional overturning circulation in a coupled climate model. Clim. Past 3, 97–107.

Shi, N., Dupont, L.M., Beug, H.-J., Schneider, R., 2000. Correlation between vegetation in southwestern Africa and oceanic upwelling in the past 21,000 years. Quat. Res. 54, 72–80.

Shinn, E.A., Reese, R.S., Reich, C.D., 1994. Fate and pathways of injection-well effluent in the Florida Keys. U.S. Geological Survey Open-File Report 94-276.

Solignac, S., de Vernal, A., Hillaire-Marcel, C., 2004. Holocene sea-surface conditions in the North Atlantic—contrasted trends and regimes in the western and eastern sectors (Labrador Sea vs. Iceland Basin). Quat. Sci. Rev. 23, 319–334.

Southon, J., Kashgarian, M., Fontugne, M., Metivier, B., Yim, W.W.-S., 2002. Marine reservoir corrections for the Indian Ocean and Southeast Asia. Radiocarbon 44, 167–180.

Stuiver, M., Pearson, G.W., Braziunas, T.F. 1986. Radiocarbon age calibration of marine samples back to 9000 cal yr BP. Radiocarbon 28(2B), 980–1021.

Swarzenski, P., 2007, U/Th series radionucleotides as coastal groundwater tracers. Chem. Rev.107, 663–674.

Thornalley, D.J.R., Elderfield, H., McCave, I.N., 2009. Holocene oscillations in temperature and salinity of the surface subpolar North Atlantic. Nature 457, 711–714.

Thornalley, D.J.R., Blaschek, M., Davies, F.J., Praetorius, S., Oppo, D.W., McManus, J.F., Hall, I.R., Kleiven, H., Renssen, H., McCave, I.N., 2013. Long-term variations in Iceland–Scotland overflow strength during the Holocene. Clim. Past 9, 2073–2084.

Törnqvist, T.E., Rosenheim, B.E., Hu, P., Fernandez, A.B., 2015. Radiocarbon dating and calibration. In Shennan, I., Long, A.J., Horton, B.P. (eds.). Handbook of Sea-Level Research. John Wiley & Sons, Oxford, p. 349–372.

Toth, L.T., Aronson, R.B., Cobb, K.M., Cheng, H., Edwards, R.L., Grothe, P.R., Sayani, H.R., 2015a. Climatic and biotic thresholds of coral-reef shutdown. Nat. Clim. Chang. 5, 369–374.

Toth, L.T., Aronson, R.B., Cheng, H., Edwards, R.L., 2015b. Holocene variability in the intensity of wind-gap upwelling in the tropical eastern Pacific. Paleoceanography 30, 1113–1131.

Toth, L.T., Stathakopoulos, A., Kuffner, I.B., 2016. Species composition of the Holocene coral reefs of the middle Florida Keys. USGS Open-File Report 2016–1074.

[dataset] Toth, L.T., Cheng, H., Edwards, R.L., Ashe, E., and Richey, J.N., 2017, Local Radiocarbon Reservoir Age (ΔR) Variability from the Nearshore and Open-Ocean Environments of the Florida Keys Reef Tract During the Holocene and Associated U-Series and Radiocarbon Data. U.S. Geological Survey Data Release, https://doi.org/10.5066/F7P8492Q.

Wagner, A.J., Guilderson, T.P., Slowey, N.C., Cole, J.E., 2009. Pre-Bomb Surface Water Radiocarbon of the Gulf of Mexico and Caribbean as Recorded in Hermatypic Corals. Radiocarbon 51, 947–954.

Wilson, W.D., Johns, W.E., 1997. Velocity structure and transport in the Windward Island Passages. Deep-Sea Res. Part I 44, 487–520.

Zaunbrecher, L.K., Cobb, K.M., Beck, J.W., Charles, C.D., Druffel, E.R.M., Fairbanks, R.G., Griffin, S., Sayani, H.R., 2010. Coral records of central tropical Pacific radiocarbon variability during the last millennium. Paleoceanography 25, PA4212.

Tables

Table 1. Corrected ^{230}Th ages, conventional ^{14}C ages, and predicted ^{14}C ages from the Marine13 calibration curve (Marine13 age) used to calculate local reservoir age (ΔR) for the coral samples (listed by Sample ID and genera). All errors are 1σ. Data ultimately excluded from the models of ΔR based on our screening procedures are indicated in red.

Region	**Subregion**	**Sample ID**	**Genus**	**^{230}Th age**	**Conventional ^{14}C age**	**Marine13 age**	**ΔR**
Open ocean	Dry Tortugas N.P.	DT-GB-3-2	*Orbicella*	156±7	465±30	543±25	**-78±38**
		DT-GB-5-0.5	*Orbicella*	590±4	970±35	998±25	**-28±43**
		DT-GB-5-2	*Colpophyllia*	1253±3	1630±35	1681±26	**-51±44**
		DT-GB-1-0	*Orbicella*	1771±12	2095±35	2169±27	**-74±44**
		DT-GB-1-2	*Orbicella*	2444±5	2775±30	2741±25	**34±39**
		DT-PB-3-0	*Orbicella*	2550±7	2825±35	2803±25	**22±43**
		DT-GB-6-0	*Orbicella*	3564±5	3675±25	3659±24	**16±35**
		DT-PB-3-14	*Colpophyllia*	3766±5	3800±30	3813±26	**-13±40**
		DT-GB-1-17	*Orbicella*	4374±7	4145±25	4243±25	**-98±35**
		DT-PB-1-4	*Orbicella*	4812±8	4490±30	4581±25	**-91±39**
		DT-GB-7-4	*Diploria*	4945±6	4665±35	4715±26	**-50±44**
		DT-LB-1-16.5	*Diploria*	5079±8	4780±25	4823±26	**-43±36**
		DT-LB-1-22	*Diploria*	5633±9	5150±30	5285±25	**-135±39**
		DT-GB-1-10	*Colpophyllia*	6096±12	5580±35	5673±28	**-93±45**
		DT-GB-7-27	*Diploria*	6503±8	5960±35	6090±27	**-130±44**
		DT-GB-1-12	*Diploria*	7424±16	6320±35	6681±28	**-361±45**
		DT-LB-1-45	*Diploria*	7432±9	6780±35	6937±27	**-157±44**
		DT-LB-1-49	*Diploria*	7825±10	7260±40	7357±26	**-97±48**
		DT-GB-1-14	*Orbicella*	7877±9	7270±35	7411±28	**-141±45**
	Marquesas	MQ-1-1	*Orbicella*	2349±7	2680±25	2690±25	**-10±35**
		MQ-8-0	*Orbicella*	3578±8	3680±25	3673±25	**7±35**
		MQ-8-25	*Montastraea*	5551±9	5115±25	5156±25	**-41±35**
		MQ-4-13	*Diploria*	7910±12	7375±20	7428±27	**-53±34**
Nearshore	Lower Keys	LK-LK-8-0	*Montastraea*	274±6	520±25	626±23	**-106±34**
		LK-LK-2-0	*Acropora*	1037±5	1510±25	1482±25	**28±35**
		LK-MG-2-0	*Montastraea*	4520±5	4605±25	4387±25	**218±35**
		LK-MG-1-0	*Orbicella*	5110±8	4840±30	4822±26	**18±40**
		LK-LK-2-10	*Acropora*	5563±8	5090±25	5104±25	**-14±35**
		LK-LK-12-0	*Diploria*	5721±9	5320±25	5365±25	**-45±35**
		LK-MG-3-2.5	*Orbicella*	6002±10	5775±25	5634±28	**141±38**
		LK-LK-12-10	*Acropora*	6399±7	6015±25	5991±27	**24±37**

	LK-LK-5-0	*Diploria*	7084±10	6560±25	6655±30	**-95±39**
	LK-MG-1-10	*Orbicella*	7191±14	6560±35	6658±31	**-98±47**
	LK-MG-1-15	*Orbicella*	7695±13	7200±25	7249±27	**-49±37**
Middle Keys	MK-SR-3-0	*Acropora*	1013±3	1415±25	1472±26	**-57±27**
	MK-AR-7-0	*Acropora*	5508±7	5535±25	5136±26	**399±29**
	MK-AR-2-0	*Acropora*	5922±10	5465±25	5108±25	**357±32**
	MK-SR-1-5	*Acropora*	6378±7	5955±30	5958±27	**-3±30**
	MK-TN-4-0	*Acropora*	6612±8	6245±25	6161±27	**84±31**
	MK-AR-2-5	*Acropora*	6921±9	6475±35	6434±26	**41±32**
	MK-TN-1-6	*Acropora*	6998±10	6505±30	6506±27	**-1±33**
	MK-SR-1-15	*Diploria*	7289±9	6795±35	6767±27	**28±32**
	MK-AR-4-10	*Diploria*	7644±8	7265±25	7179±28	**86±32**
Upper Keys	UK-GR-5-0	*Acropora*	41±4	380±35	448±23	**-68±42**
	UK-GR-5-10	*Acropora*	1201±4	1520±30	1627±25	**-107±39**
	UK-GR-3-0	*Diploria*	1234±7	1615±25	1658±26	**-43±36**
	UK-GR-3-5	*Montastraea*	1326±6	1765±25	1793±26	**-28±36**
	UK-CF-HM-7	*Acropora*	1937±4	2275±25	2326±25	**-51±35**
	UK-GR-4-0	*Orbicella*	2233±4	2425±25	2540±26	**-115±36**
	UK-CF-7-1	*Acropora*	2873±6	3165±25	3111±27	**54±37**
	UK-GR-4-10	*Orbicella*	4979±12	4750±25	4750±25	**0±35**
	UK-CF-1-15	*Acropora*	5777±28	5340±25	5415±26	**-75±36**
	UK-GR-4-24	*Orbicella*	6030±10	5665±30	5650±27	**15±40**
	UK-CR-1-1	*Acropora*	6241±9	5790±25	5804±27	**-14±37**
	UK-KL-5-14	*Diploria*	6739±8	6350±30	6291±28	**59±41**
	UK-CR-2-10	*Orbicella*	6822±13	6375±25	6352±26	**23±36**
	UK-CF-HM-64	*Orbicella*	7479±10	6890±25	6986±27	**-96±37**
Biscayne N.P.	BP-PR-1-2	*Orbicella*	1009±4	1510±70	1470±26	**40±75**
	BP-AR-1-0.4	*Orbicella*	1808±6	2190±60	2201±27	**-11±66**
	BP-AR-2-1.5	*Orbicella*	2850±6	3065±30	3088±27	**-23±40**
	BP-AR-4-3	*Colpophyllia*	4518±7	4285±25	4384±25	**-99±35**
	BP-AR-3-3	*Orbicella*	5455±7	5155±30	5091±25	**64±39**
	BP-LR-2-0	*Acropora*	5501±8	5150±25	5135±25	**15±35**
	BP-AR-6-6	*Diploria*	6543±9	6075±35	6115±26	**-40±44**
	BP-FR-2-10	*Orbicella*	7998±12	7450±30	7554±28	**-104±41**
	BP-FR-1-11	*Acropora*	8600±11	8070±60	8150±27	**-80±66**
	BP-FR-2-20	*Acropora*	9443±11	8760±25	8763±29	**-3±38**
	BP-FR-2-55	*Diploria*	10242±12	9485±25	9438±27	**47±37**

Table 2. Comparison between the Holocene average ΔR and modern ΔR for the open-ocean and nearshore locations on the FKRT from this study to values of ΔR from elsewhere in the western Atlantic from the Marine Reservoir Database (http://calib.qub.ac.uk/marine/; Reimer and Reimer, 2001). Where multiple values were available from a location (*), we present a weighted mean ± 1σ.

Location	*ΔR (±1σ)*	*Reference*
Open ocean (Holocene)	-64±27	This study
Open ocean (modern)	-60±33	This study
Nearshore (Holocene)	-25±20	This study
Nearshore (modern)	-53±32	This study
Bahamas*	-8±64	Broecker and Olson, 1961
Jamaica*	-37±29	Broecker and Olson, 1961
Flower Garden Banks	-30±9	Wagner et al., 2009
Puerto Rico	-27±24	Kilbourne et al., 2007
Mexico*	-32±19	Wagner et al., 2009
Bermuda	-129±29	Druffel, 1997a
Venezuela*	-28±5	Guilderson et al., 2005; Wagner et al., 2009

Figure Captions

Figure 1. (a) Generalized depiction of the major currents of the Atlantic (solid lines): Gulf Stream (GS), North Atlantic Drift (NAD), Canary Current upwelling system (CC(u)), North Equatorial Current (NEC), Equatorial Counter Current (ECC), South Equatorial Current (SEC), Benguela Current upwelling system (BC(u)), and Brazilian Current (BC). The locations of North Atlantic Deepwater Formation (NADW) in the Labrador and Nordic Seas are indicated by dashed lines. The currents not discussed specifically in the text are in gray. The shaded rectangle in (a) indicates the bounds of (b), the location of the study area in relation to the major currents of the Caribbean: Caribbean current (CC), Yucatan current (YC), Loop Current (LC), Florida Current (FC), and Gulf Stream (GS) drawn after Gyory et al. (2013). The shaded rectangle in (b) indicates the location of the study, (c). Sampling locations along the FKRT (black shading; from the benthic habitat maps derived by Florida Fish and Wildlife Conservation Commission-Fish and Wildlife Research Institute, National Oceanic and Atmospheric Administration Coastal

Services Center, Dade County, FL (http://ocean.floridamarine.org/metadata/custom/SECOORA/south_fl_coral_reefs.htm) are indicated by white circles. Dashed lines within the FKNMS show the boundaries between subregions of the FKRT (after Klein and Orlando, 1994). Black arrows indicate locations where water flows from Florida and Biscayne Bays onto the reef.

Figure 2. Modeled ΔR over time (^{230}Th age; solid line) with 1σ (dark shading) and 2σ (light shading) uncertainties for (a) the open-ocean (blue; 8000 yrs BP to present) and (b) the nearshore (red; 9500 yrs BP to present) environments of the FKRT. Colored bars represent the coral-based snapshots of ΔR from the Dry Tortugas N.P. (blue), Marquesas (cyan), Keys (red), and Biscayne N.P. (orange) subregions of the FKRT. The width of each bar represents the 2σ range of the ^{230}Th age of the coral and the height of each bar represents the 2σ uncertainty of the estimate of ΔR from that coral. (c) Provides a direct comparison of modeled ΔR variability from open-ocean (blue) and nearshore (red) locations.

Figure 3. Comparison between (a) modeled variability in ΔR from open-ocean (blue) and nearshore (red) environments with 1σ (dark shading) and 2σ (light shading) uncertainties and paleoceanographic reconstructions from the Straits of Florida based on the geochemistry of the planktonic foraminifera G. ruber. (b) G. ruber $\delta^{18}O$ from core 79GGC (Lund and Curry, 2004). (c) G. ruber Mg/Ca from core JPC51 (Schmidt et al., 2012). (d) $\delta^{18}O_{sw}$ derived from G. ruber $\delta^{18}O$ and Mg/Ca in core JPC51 (Schmidt et al., 2012). Dark lines represent 1000 y running means of the raw data and light lines represent 200-year running means. Triangles indicate the median calibrated ^{14}C ages used to create the age models of the records.

Figure 4. Calibrated calendar ages BP, where present is 1950 (cal BP; black points) and 2σ ranges of those calibrations for the conventional radiocarbon age, 5960±35, of a coral sample from Dry Tortugas N.P. plotted with the "true" (^{230}Th) age (dashed line) with 2σ error (gray shading) of that same coral. The conventional radiocarbon age was calibrated to cal BP using ΔR from three published estimates of ΔR from the FKRT: 1) a living coral colony collected from the Dry Tortugas N.P. in 1884 (ΔR=114±51; Lighty, 1982; Reimer and Reimer, 2001), 2) average values from 1945 to 1950 AD from living corals from the Upper Keys (ΔR=3±13; Druffel and Linick, 1978; Druffel, 1997a; Reimer and Reimer, 2001), 3) a weighted mean of these two values (ΔR=40±33; Reimer and Reimer, 2001) and two modeled estimates of open ocean ΔR: 1) the modern value from our model (ΔR=-64±27), and 2) the age-specific model prediction for the conventional ^{14}C age of the coral (ΔR=-104±25).

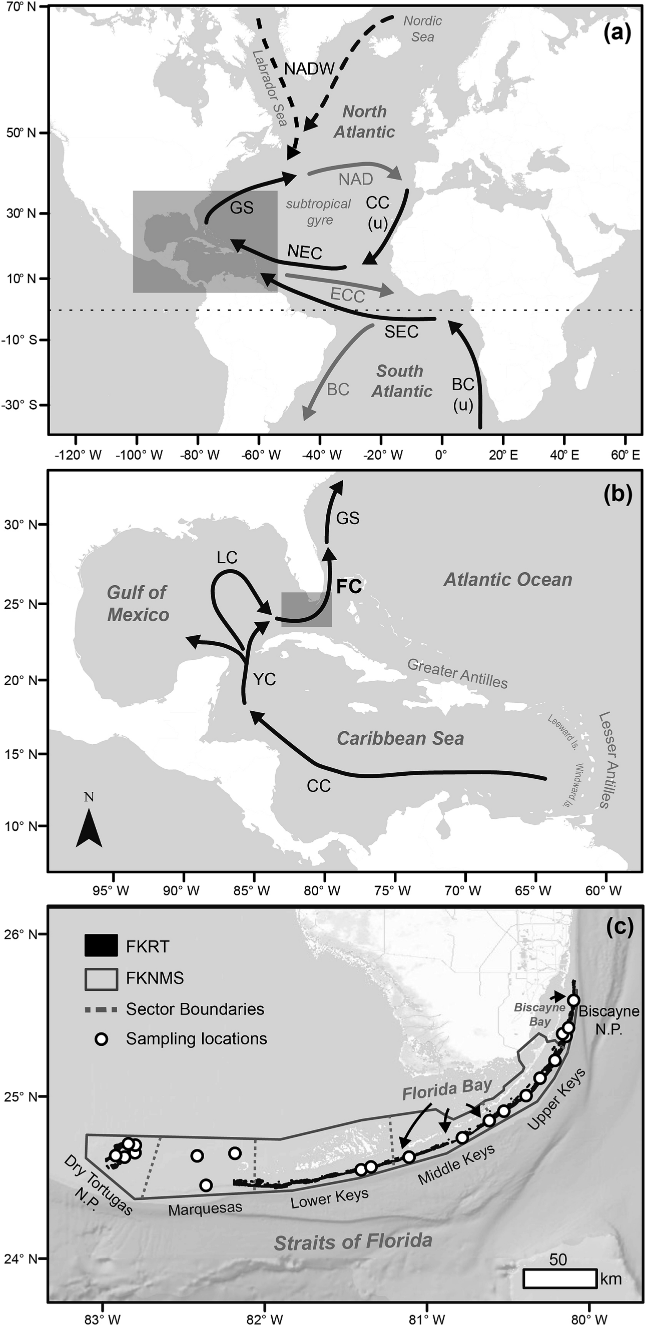

(a)
70° N
50° N
30° N
10° N
-10° S
-30° S
Nordic Sea
Labrador Sea
NADW
North Atlantic
NAD
GS
subtropical gyre
CC (u)
NEC
ECC
SEC
South Atlantic
BC
BC (u)
-120° W
-100° W
-80° W
-60° W
-40° W
-20° W
0°
20° E
40° E
60° E
(b)
30° N
25° N
20° N
15° N
10° N
GS
LC
FC
Atlantic Ocean
Gulf of Mexico
YC
Greater Antilles
Caribbean Sea
Leeward Is.
Windward Is.
Lesser Antilles
CC
N
95° W
90° W
85° W
80° W
75° W
70° W
65° W
60° W
(c)
26° N
25° N
24° N
FKRT
FKNMS
Sector Boundaries
Sampling locations
Biscayne Bay
Biscayne N.P.
Florida Bay
Upper Keys
Middle Keys
Lower Keys
Marquesas
Dry Tortugas N.P.
Straits of Florida
50
km
83° W
82° W
81° W
80° W

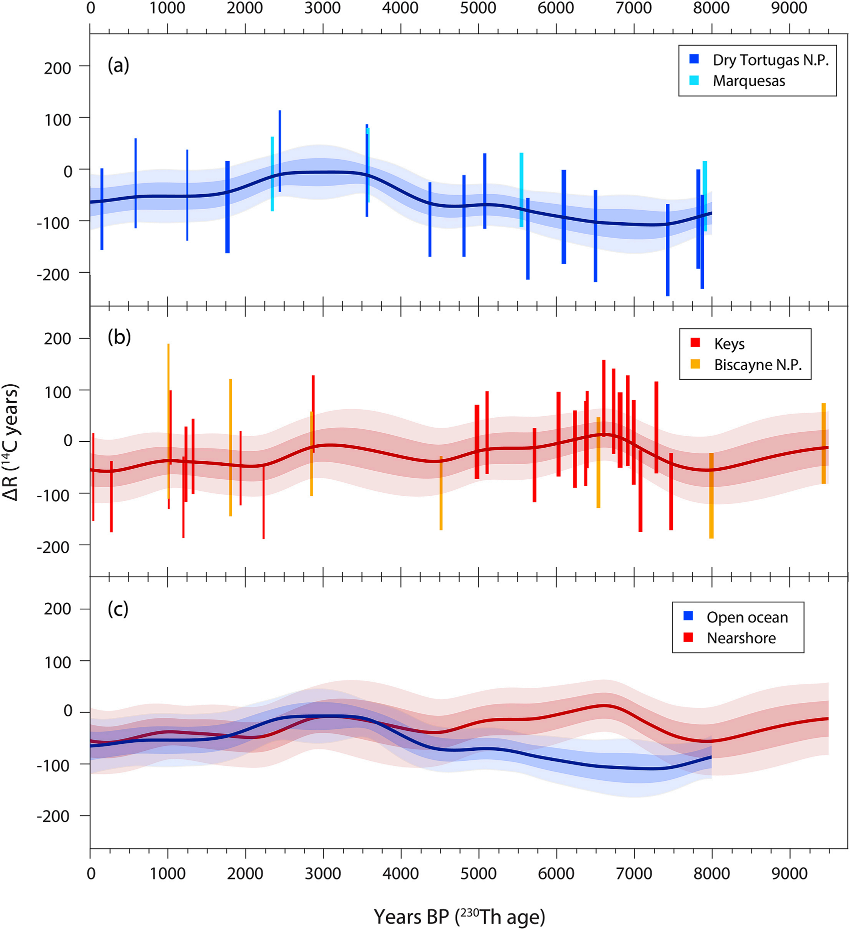

(a)
Dry Tortugas N.P.
Marquesas
(b)
Keys
Biscayne N.P.
(c)
Open ocean
Nearshore
ΔR (14C years)
Years BP (230Th age)
200
100
0
-100
-200
0
1000
2000
3000
4000
5000
6000
7000
8000
9000

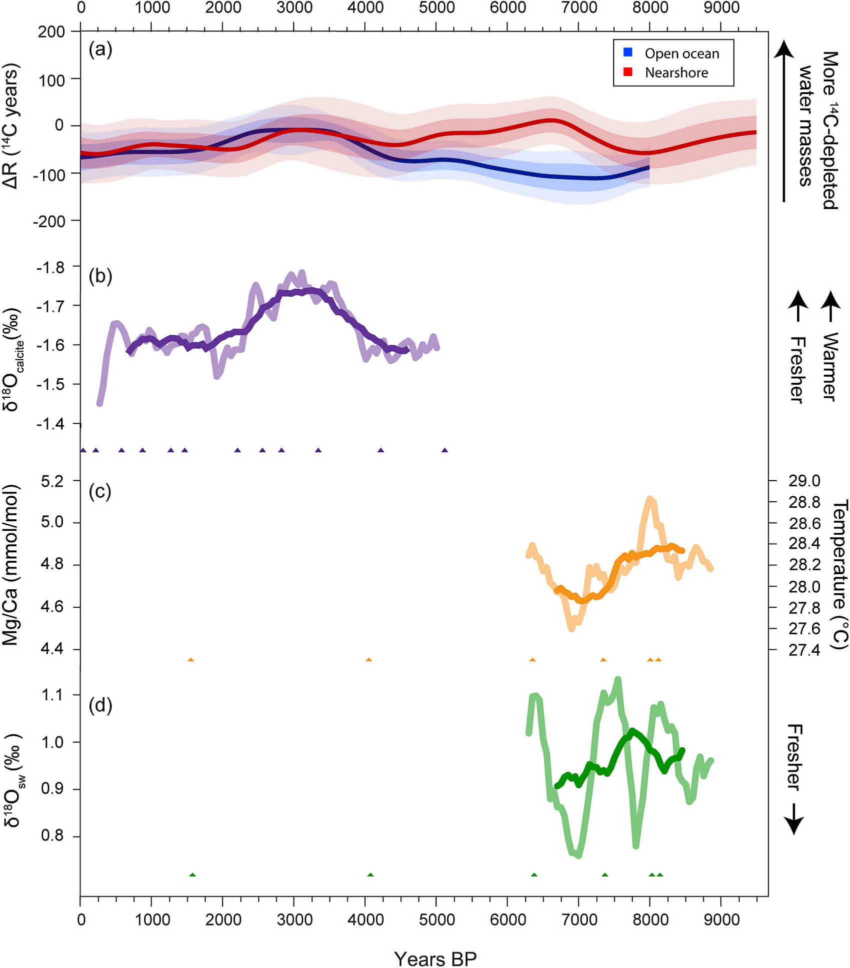

(a)
Open ocean
Nearshore
ΔR (14C years)
More 14C-depleted water masses
(b)
δ18Ocalcite(‰)
Fresher
Warmer
(c)
Mg/Ca (mmol/mol)
Temperature (°C)
(d)
δ18Osw (‰)
Fresher
Years BP

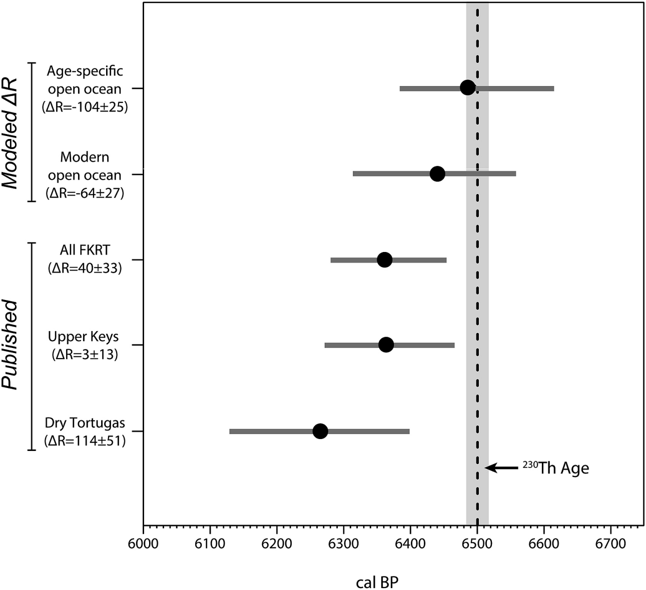
Modeled ΔR
Age-specific
open ocean
(ΔR=-104±25)
Modern
open ocean
(ΔR=-64±27)
Published
All FKRT
(ΔR=40±33)
Upper Keys
(ΔR=3±13)
Dry Tortugas
(ΔR=114±51)
230Th Age
6000
6100
6200
6300
6400
6500
6600
6700
cal BP